

CARBON AND WATER CYCLING IN A TEXAS HILL COUNTRY WOODLAND

A Dissertation

by

RAY HERBERT KAMPS

Submitted to the Office of Graduate and Professional Studies of  
Texas A&M University  
in partial fulfillment of the requirements for the degree of

DOCTOR OF PHILOSOPHY

Chair of Committee,  
Committee Members,

James Heilman  
Kevin McInnes  
Georgianne Moore  
Charles Lafon

Interdisciplinary Program  
Chair,

Ronald Kaiser

December 2014

Major Subject: Water Management and Hydrological Science

Copyright 2014 Ray Herbert Kamps

## ABSTRACT

Two tree species, Plateau live oak (*Quercus fusiformis*) and Ashe juniper (*Juniperus ashei*) survive and thrive in a dense woodland on thin soil overlying massive limestone formations in the Texas Hill Country with recurrent annual summer drought punctuated every few years by intense rain and flooding. Previous research has shown that these species exhibit nearly opposite drought survival strategies at the root, stem and leaf levels. A fundamental question developed as to how these two apparently co-dominant species partition the scarce water resource under varying annual precipitation patterns. Eddy covariance and dendrochronology techniques were used to investigate carbon and water cycling from 2004 to 2012 in this setting. Essential information on the forest canopy age and species composition was obtained from a line-transect survey coupled with the bootstrap statistical method. Interannual change in water storage masked the relationships between annual precipitation and both annual evapotranspiration and annual productivity. A pair of methods were developed to minimize this masking effect caused by the interannual change in water storage using sequential linear regressions of annual precipitation versus ET or GPP by optimizing the start date of the annual timeframe as well as making a lag adjustment to the data for best goodness of fit.

The oaks and junipers were found to be co-dominant in the woodland canopy by number, each composing approximately 50%. Juniper was clearly dominant in the understory at 76%, while oak was clearly dominant in terms of carbon flux (80%) and

standing biomass (85%). Evapotranspiration accounted for 72% of the fate of annual precipitation and the oaks are presumed to be the greatest water users due to the link between carbon and water fluxes through stomatal conductance.

Using October 1<sup>st</sup> (calendar day 274) as the start date for mass balance determination minimized the effect of the change in storage of plant-available water for both evapotranspiration and carbon flux. The optimal lag adjustment for evapotranspiration was 95 days while that of carbon flux was 91 days. These methods increased the ability of annual precipitation to explain the water and carbon budgets to 97% (up from 59%) and 96% (up from 64%) respectively. In this ecosystem, this demonstrated that most of the remaining variation when using the calendar year is a function of storage capacity and an artifact of timing.

## DEDICATION

For of Him, and through Him, and to Him, are all things: to Whom be glory for ever. Amen. Romans 11:36 KJV

## ACKNOWLEDGEMENTS

I wish to acknowledge the influence and encouragement of my parents, Rev. John Herbert Kamps, Ph.D and Mrs. Mary Ruth (Sleight) Kamps or "Dad and Mom" as I know them. They always encouraged me to further my education during my formative years. While my dad was alive, he said, "Always be working on the next degree." He graduated with his Ph.D. at age 64. My mom also has always encouraged me to pursue a Ph.D. and is looking forward to graduation day when I follow his example.

To my wife, Janet Riggs Kamps: Thank you, thank you, thank you for your support. You are an incredible person. I love you. Now it is your turn to get a doctorate.

This being the culmination my academic pathway as a student, I wish to thank the many professors of my undergraduate years with particular thanks to: Dr. Tang (Chemistry), Dr. Archer (Ecology), Dr. Ellison (Genetics), Dr. Mueller (Botany).

Dr. Michael Speed, Sr. (Statistics) and Dr. James Cotner (Limnology) stand out as significant teachers during my Master of Science program.

In my first attempt at a doctoral program at Texas State University, Dr. Vince Lopes (Hydrology) and Mr. Joe Grady Moore, Jr. (Water Policy) deserve special appreciation. Dr. Klein (Digital image interpretation and Geomorphology) and Dr. Popescu stand out during my second doctoral program at Texas A&M University.

Appreciation is extended to two members of my graduate committee here at Texas A&M University for being my teachers and mentors: Dr. Charles Lafon and Dr. Georgianne Moore.

I wish to thank my graduate advisors: Dr. William H. Neill for my Master's program, Dr. Alan Groeger for my doctoral program at Texas State University, and Dr. James L. Heilman for my current doctoral program.

A word of apology is warranted to Dr. Groeger for my withdrawing from my first doctoral program due to familial and personal exigencies and for failing to return to finish the program when the problems were resolved. You deserved better than that. I deeply apologize and thank you for remaining my friend.

This research was funded in part by research grants from NASA and the US Department of Energy.

## TABLE OF CONTENTS

	Page
ABSTRACT .....	ii
DEDICATION .....	iv
ACKNOWLEDGEMENTS .....	v
TABLE OF CONTENTS .....	vii
LIST OF FIGURES .....	x
LIST OF TABLES .....	xii
CHAPTER I INTRODUCTION AND LITERATURE REVIEW .....	1
Introduction .....	1
Literature Review .....	7
Tree responses to climate .....	7
Dendrochronology applications .....	8
Eddy covariance applications .....	8
Linkage studies .....	10
CHAPTER II FOREST SPECIES-AGE STRUCTURE IMPACT ON CARBON ASSIMILATION .....	12
Introduction .....	12
Methods .....	14
Sampling plan .....	14
Field measurements .....	15
Density calculations .....	16
Dendrochronology of juniper .....	20
Dendrochronology of oak .....	21
Biomass calculations .....	22
Results .....	23
Tree density .....	23
Dendrochronology .....	26
Biomass calculations .....	27
Discussion .....	30
Conclusions .....	34

	Page
CHAPTER III EMPIRICAL CALCULATION OF THE WATER YEAR IN SUB-TROPICAL, SEMI-ARID FORESTS .....	35
Introduction .....	35
Methods .....	37
Site description .....	37
Precipitation and flux measurements .....	38
Annual data and best fit day of year .....	39
Lag adjustment .....	41
Results .....	41
Start date determination .....	41
Lagging .....	41
Discussion .....	42
Conclusions .....	48
CHAPTER IV A GENERALIZED METHOD FOR DETERMINING A HYDRO-ECOLOGICAL YEAR AND OPTIMIZING FOR ECOSYSTEM LAG .....	50
Introduction .....	50
Methods .....	54
Site description .....	54
Precipitation and flux measurements .....	55
Annual data and determination of best fit start day of HEY .....	57
Lag adjustment .....	58
Results .....	58
Start date determination .....	58
Lagging .....	60
Rain use efficiency .....	62
Discussion .....	62
Conclusion .....	66
CHAPTER V CARBON FLUX PARTITIONING BETWEEN TWO SPECIES IN A RAPIDLY CHANGING FOREST .....	67
Introduction .....	67
Methods .....	72
Eddy covariance estimate of NEP .....	72
Dendrochronological estimates of wood increment .....	72
Light study .....	73
Results .....	74
Discussion .....	74
NEP .....	78

	Page
Biometric measurements .....	78
Conclusions .....	80
CHAPTER VI CONCLUSIONS .....	83
Relationship to Previous Studies .....	83
Broader Implications .....	85
Future Directions .....	86
REFERENCES .....	87
APPENDIX A VALIDATION STUDY .....	99
APPENDIX B MONTHLY DATA VALUES.....	104

## LIST OF FIGURES

	Page
Fig. 1.1 Freeman Ranch. ....	5
Fig. 1.2 Location map in Texas.....	6
Fig. 2.1 Example bootstrap procedure carried out to 1000 iterations. ....	19
Fig. 2.2 Age structure of the two dominant canopy species. ....	28
Fig. 2.3 Tree radii history at dbh. ....	28
Fig. 2.4 Biomass plots to estimate parameters for equations by Jenkins et al. (2003).....	29
Fig. 2.5 Biomass history of the study trees. ....	29
Fig. 2.6 Biomass history extrapolated to a per hectare basis. ....	30
Fig. 3.1 Coefficient of determination between AP and AET. ....	42
Fig. 3.2 Graph showing the lag between AP and AET.....	43
Fig. 3.3 Improvement in goodness of fit when lagging AET by 95 days. ....	43
Fig. 3.4 Correlation between annual precipitation and annual ET as a function of lag time. ....	44
Fig. 3.5 Runoff + percolation as a function of AP. ....	47
Fig. 4.1 Comparison of AGPP and AP for the calendar year and the USGS water year. ....	59
Fig. 4.2 Correlation of annual precipitation and annual GPP with lagging. ....	60
Fig. 4.3 Comparison of unlagged annual GPP and annual precipitation (a), and lagged annual GPP and annual precipitation (b). ....	61
Fig. 4.4 Coefficient of determination throughout the calendar year between AP and AGPP.....	61
Fig. 4.5 Annual rain use efficiency as a function of annual precipitation.....	63
Fig. 5.1 Carbon sequestration estimates.....	75

	Page
Fig. 5.2 Partitioning and scaling of NEP components. ....	75
Fig. 5.3 Carbon balance of eddy covariance measurements. ....	76

## LIST OF TABLES

	Page
Table 2.1 Example of bootstrap operation. ....	18
Table 2.2 Data and results for the two variations of the nearest neighbor estimates (NN and NN2) using species-specific data. ....	25
Table 2.3 Data and results for the NN2 calculation of density using pooled data and assuming a non-random but even distribution of trees. ....	25
Table 2.4 Partitioning tree density into species density. ....	26
Table 3.1 Annualized data.....	48
Table 5.1 Situational sources of error when using eddy covariance. ....	71

## CHAPTER I

### INTRODUCTION AND LITERATURE REVIEW

#### **Introduction**

Densely wooded areas composed mainly of Plateau live oak (*Quercus fusiformis*) and Ashe juniper (*Juniperus ashei*) survive and thrive in thin soils overlying limestone bedrock in the Texas Hill Country despite recurrent droughts punctuated every few years by intense rains and flooding (Slade, 1986). A fundamental question develops as to how these two apparently co-dominant trees partition the scarce water resource. Juniper are drought tolerators (Eggemeyer and Schwinning, 2009), wringing the maximal amount of moisture out of the soil, using all that is available and matching their physiologic functions to water availability. In terms of their leaf water potential, they appear to be anisohydric, maintaining gas exchange while leaf water potential drops (McDowell et al., 2008). This strategy avoids carbon starvation while risking excessive water loss from the leaves and hydraulic failure due to embolism in the trunk and branches (McDowell et al., 2008). Many oaks are known to be phreatophytes, that is, deeply rooted into saturation zones, as illustrated in Miller (2009) for Blue oaks (*Q. douglasii*). However, Eggemeyer and Schwinning (2009) showed that neither the more deeply rooted mesquite nor the more shallowly rooted juniper have access to a stable supply of water in the Texas Hill Country, based upon isotopic enrichment of  $^2\text{H}$  and  $^{18}\text{O}$  due to evaporation. It therefore seems unlikely that the Plateau live oaks are able to avoid the

effects of drought using the phreatophyte strategy in this area because saturated ground water is simply too deep to tap, although they are more deeply rooted than the junipers and have access to somewhat deeper water sources (Schwinning, 2008). Bendevis et al. (2009) in a year-long leaf-level study, also in the Texas Hill Country found that Plateau live oaks excelled at carbon exchange and stomatal regulation while the junipers exhibited higher water use efficiency. This means that the oaks are isohydric (McDowell et al., 2008), maintaining leaf water potential at the expense of photosynthesis under water stress, effectively trading sugar for water with the consequence that all forms of carbohydrate production, both energy and structural carbohydrates will diminish or cease. From this, Bendevis et al. (2009) inferred that the two species are approximately competitively equal at the leaf-level.

Conifers such as juniper rely on relatively small diameter tracheids for water transport from root to shoot while woody angiosperms have both tracheids and the much larger vessel elements which appear as pores in microscopic cross-sectional analysis (Meinzer et al., 2013; Sperry et al., 1994). Angiosperm tree species are generally divided into ring-porous and diffuse-porous species where the ring-porous species produce large vessels early in the growing season, followed by sparse, small vessels throughout the rest of the growing season. Diffuse porous species produce many small vessels through the growing season (Taneda and Sperry, 2008). Plateau live oak produces both large-early vessels and densely packed small vessels throughout the growing season. Each large vessel can conduct the equivalent of 10 small vessels (Hacke et al., 2006), but is more prone to embolism in both summer drought and winter

freezing (Taneda and Sperry, 2008). It is unknown how the use of both strategies benefits this live oak species.

Given that the water management mechanisms are so different at the root, stem and leaf levels, then the approximate competitive equality found by Bendevis et al. (2009) may be confined to the single year of study and may not be the case under other precipitation patterns. Also, the area of the live oaks is fairly constant while the area of the junipers is rapidly expanding (Bendevis et al., 2009). This is not explained by the one-year, leaf-level investigation but requires a multi-year investigation with a broader scope. Two techniques which can provide multi-year perspective and a broad scope are dendroclimatology and eddy covariance which operate at the tree (and by extension, population) and ecosystem levels, respectively.

Eddy covariance techniques can be used to measure the net ecosystem exchange (NEE) of atmospheric carbon dioxide and water use while the plants are alive and without damaging them. Techniques exist to separate respiration and photosynthesis components of NEE, thereby enabling the primary producer's immediate response to their environment to be described. Dendroclimatology measures each year's increase of a tree's radius after the growth of interest is finished. It is a very direct method of measuring a plant's long term response to its environment. This is accomplished by either measuring annual rings in a core taken out of the tree of interest (leaving a hole where the sample was removed) or felling the tree and measuring annual rings in the cross section. The most likely driver of annual ring width variation from year to year is annual precipitation which can vary across a wide range of values. Purely physiological

changes are more likely to be incremental and unidirectional, such as the consistent decrease in ring width with age. Annual ring width variation due to competition for resources (other than water) are likewise incremental while variation caused by disease and parasite tend to be isolated. Eddy covariance and dendroclimatology are two well established techniques with extensive literature backgrounds, addressing similar questions at different scales.

The central question of this dissertation is to what extent these two species which are apparently co-dominant in areal coverage and reportedly equal competitors at the leaf level are also co-dominant in water and carbon cycling at the landscape level. Determining the species specific contribution to the water and carbon cycles required several steps, each of which takes the form of a chapter in this dissertation.

The age and species mix of the forest are determined by transect sampling and dendrochronology in Chapter II along with an estimate of standing biomass and annual biomass increment for each species. In dendrochronology, the annual timeframe is determined by the timing of the formation of annual rings in the tree trunks. There is nothing in the tree rings themselves to indicate whether this is January 1<sup>st</sup> to December 31<sup>st</sup> or any other possible year. An appropriate annual timeframe is developed from eddy covariance and precipitation data for evapotranspiration (ET) in Chapter III and from Gross Primary Productivity (GPP) in Chapter IV. The closure of mass balance for water is facilitated in Chapter III by the stimulus (precipitation) and response (ET) both being water. No such closure is possible between precipitation and GPP for carbon in Chapter IV. Therefore, the mass balance of carbon in the ecosystem is addressed in

Chapter V, in particular, the relationship between the two codominant species and carbon cycling. Chapters II to V are each written as independent articles with the exception that the methods section in Chapter V uses similar or identical methods to those used in Chapter II and Chapter IV and incorporates them by reference rather than restating them. Chapter VI develops synergisms from the previous chapters, identifies deficiencies and suggests new directions in the research.



**Fig. 1.1 Freeman Ranch. The study area is indicated by a red x. Color imagery provided by Capital Area Council of Governments (CAPCOG) at: <http://www.capcog.org/data-maps-and-reports/geospatial-data/>**

The study area is the Freeman Ranch (Fig 1.1) in the Texas Hill Country near San Marcos, Texas (Fig 1.2). The ranch is on the eastern edge of the original Edwards Plateau, but this part of the Plateau is considered its own ecoregion due to the action of erosion removing the Edwardian stratum and creating deep dissections not characteristic of the Edwards Plateau proper which now starts to the west. The long term average rainfall for the study area is 858 mm (Heilman et al., 2009). The area is noted for particularly violent storms and flash floods due to warm, moist air masses from the Gulf

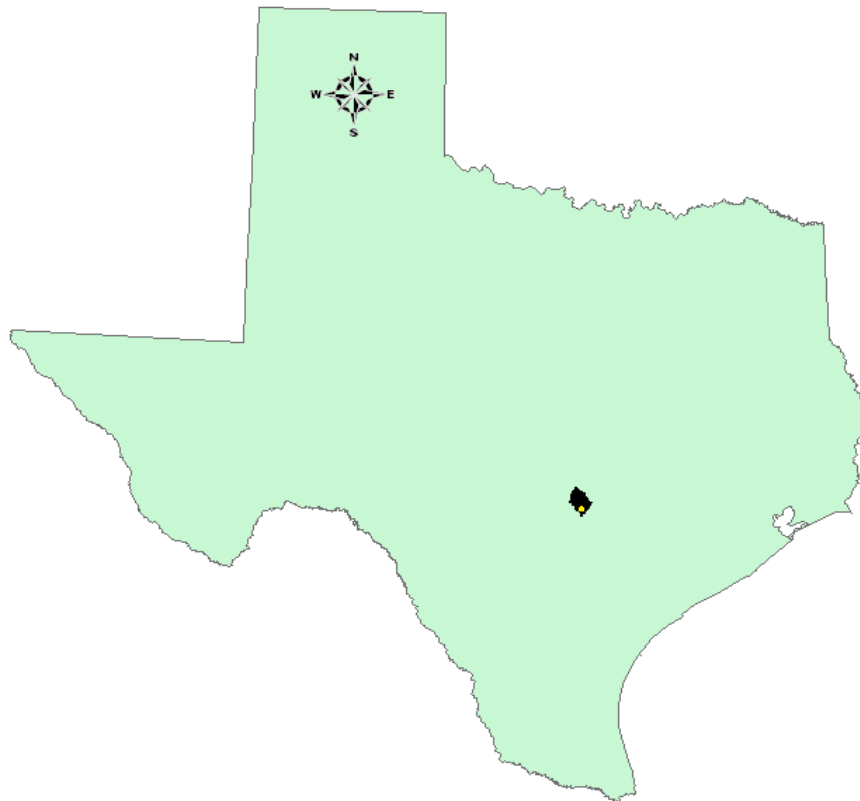


**Fig. 1.2 Location map in Texas. Hays County is silhouetted in black and San Marcos is a gold circle within Hays County. Texas and Hays County shapefiles provided by the Texas Strategic Mapping Program (StratMap) and available from: <http://www.tnris.org/get-data>**

of Mexico being lifted and redirected by the Balcones Escarpment (Slade, 1986). Three slow-release dams have been constructed in Hays County to control flash flooding, including one on Freeman Ranch. Freeman Ranch is an approximately 1700 ha ranch managed for livestock, hunting, education and research by Texas State University—San Marcos. It has a mix of grassy, shrubby and wooded areas. The eddy covariance tower (29° 56.50' N, 97° 59.49' W) at the focus of this research is surrounded by an almost unbroken 8 meter high canopy formed by Plateau live oak and Ashe juniper. Occasional individuals of cedar elm contribute to the canopy in this area as well. In other areas of the ranch, Pecan, Mesquite, Hackberry, Huisache and Black persimmon contribute a significant percentage of the tree population.

## **Literature Review**

### *Tree responses to climate*

That trees respond to their environment is basic to dendroclimatology, but there can be many climate variables (including microclimate) that trees respond to by varying the widths of their rings, such as light availability, temperature, precipitation and nutrient availability (Luckman, 2007). Precipitation is the variable of interest in this study which uses precipitation recorded at the eddy covariance tower from 2004-2013 as well as a century of rainfall records from nearby Wimberly, Texas. Unfortunately, neither of the species in this investigation has an entry in the International Tree Ring Database (NCDC, 2014). Both *Quercus* and *Juniperus* are well represented, but not *Q. fusiformis* (or *Q. virginiana*) or *J. ashei*. Also, Grissino-Mayer (1993) does not list *Q. fusiformis*

(or *Q. virginiana*) or *J. ashei*. Therefore only general trends may be gleaned from literature and specific techniques had to be developed *de novo*.

Morino (2008) showed that false rings were formed in response to drought conditions in ash and willow. This is potentially important for comparison to *J. ashei* which also forms false rings. Bartens et al. (2012) developed a method for reading ring chronologies and relating them to climate for *Q. virginiana*, a close relative of *Q. fusiformis*. Hawley (1937) was an early investigator into the relationship between juniper growth and precipitation, although a different juniper than in this study. White et al. (2011) investigated the relationship between climate and *Q. spp.* across several southern United States.

#### *Dendrochronology applications*

Cook (1985), Cook et al. (1996; 1999), Cleaveland (2000), Cleaveland and Stahle (1989) and Cleaveland et al. (1992; 2003) are a few of the many examples of climate reconstruction based on tree-ring dendroclimatology. Luckman (2007) provides a concise overview of methods. Grissino-Mayer (2001) gives a step-by-step procedural guide for analysis using the software COFECHA.

#### *Eddy covariance applications*

Baldocchi (1994; 2003) and Burba (2013) provide a detailed discussion of the eddy covariance method and applications while Kim et al. (2006) provide a more concise discussion. Heilman et al. (2009) and Kjelgaard et al. (2008) describe the method as implemented at Freeman Ranch. Rebmann et al. (2005), Baldocchi (1997) and Schmid (2002) make the case for and describe how to perform eddy covariance

tower footprint analysis. Twine et al. (2000) and Wilson et al. (2002) describe energy balance closure methods. Reichstein et al. (2005) offer a method on partitioning NEE into assimilation and respiration. Massman and Lee (2002) describe some of the uncertainties associated with long-term eddy covariance studies.

There are several software choices for processing the 10Hz raw data into meaningful fluxes and three different programs have been used to date for processing parts of the available data for other projects, all three of which were proprietary. Mauder et al. (2008) reviewed several popular software packages and had a particularly high regard for EdiRe. As of the writing of this dissertation, EdiRe is available by free download and some examples are available for developing the processing instruction set that is the heart of the program. Because of this, it was possible to develop a processing instruction set specific to the forest site data that was used in this dissertation. Mauder et al. (2008) demonstrated that differences do exist in the final product between these available software packages. Presumably this is generally true and so it seemed prudent that all data for the forest site should be processed by the same program, including that which has already been processed by the proprietary programs. A more recent entry (2011) into the free software alternatives market is EddyPro by LiCor (Lincoln, NE). In side-by-side comparisons on the forest site data with the 3 proprietary software programs and with EdiRe running an in-house developed instruction stack, EddyPro proved to be better documented, more stable, easier to use and able to give equivalent results. Because of this, EddyPro was chosen as the main processing program and the others

were used for comparison. EddyPro is not able to generate a spatially explicit flux footprint and so EdiRe was used for this purpose.

### *Linkage studies*

Curtis et al. (2002) studied correlations between eddy covariance and biometric measurements including direct trunk measurements and leaf litter measurements. Miller et al. (2004) performed a similar study with tropical forests and concluded that eddy covariance method by itself performed poorly in tropical forests and should be paired with biometric measurements. Baldocchi (1997) related drought with a decrease in NEE of carbon dioxide. However, Kljun et al. (2006) caution that local rain events at critical times or an abnormally warm spring can mitigate the effects of a regional drought on NEE. Baldocchi's paper reported carbon dynamics as NEE of CO<sub>2</sub> ranging from approximately  $-5 \text{ umol m}^{-2} \text{ s}^{-1}$  at night to  $20 \text{ umol m}^{-2} \text{ s}^{-1}$  during the day. Kljun et al. (2006) reported carbon dynamics as Net Ecosystem Productivity (NEP) in  $\text{gC m}^{-2} \text{d}^{-1}$  from -2 in the winter to approximately 6 in the summer and annual cumulative NEP in  $\text{gC m}^{-2}$  between approximately 0 (for the site hardest hit by the drought) and 400 (for the least affected). Arneth et al. (1998) also found a correlation between rainfall and carbon exchange and had yet another set of units, reporting about  $8 \text{ to } 10 \text{ Mg ha}^{-1} \text{ year}^{-1}$ . Black et al. (2007) reported in a range of  $7.30 \text{ to } 11.44 \text{ t C ha}^{-1} \text{ year}^{-1}$ . Of these studies, Baldocchi (1997) is the most pertinent to the present proposal because of its proximity and species mix. In particular, he addresses some aspects of isohydry in oaks, although without using the term "isohydry." Kim et al. (2006) linked eddy covariance measurements with estimates made using satellite remote sensing techniques. Rocha et

al. (2006) linked eddy covariance and dendrochronology. Gough et al. (2008) noted that short term comparisons between eddy covariance and biometric measurements were often poorly correlated, but tended to converge in longer term studies. Granier et al. (1996) compared results from a “one propeller eddy correlation” (OPEC) system with two types of sap flow measurements.

## CHAPTER II

### FOREST SPECIES-AGE STRUCTURE IMPACT ON CARBON ASSIMILATION

#### **Introduction**

Research into forest carbon and water dynamics at Freeman Ranch near San Marcos, Texas, USA, was conducted from 2004 to 2014 using eddy covariance techniques. Eddy covariance equipment was positioned on a tower at 14 m above ground level and 6 m above the canopy. This technique is a whole-ecosystem tool for research into net flux of carbon dioxide, water and energy and derivatives such as gross primary production, evapotranspiration and respiration, but reveals little of the drivers for these processes. It is also not useful for determining carbon sequestration, except to provide an upper bound for what is possible to sequester. The last biotic component to influence the rising eddies measured by the eddy covariance equipment is the canopy. Canopy-forming trees also intercept the majority of the available light and therefore account for the majority of the primary production and evapotranspiration (ET). Montgomery and Chazdon (2002) used 0.2 to 6.5% of full sun exposure as a normal range of light encountered by seedlings growing under a closed canopy, the rest being intercepted by the canopy. Determining the species composition and age of canopy-forming trees is important to understanding carbon and water cycling of the ecosystem.

Tree ring dating (dendrochronology) can be useful for determining age structure and biomass history of a forest canopy. Species especially suitable for

dendrochronology are those which form distinct annual rings which are concentric and easily discernable. Trees growing on the edge of their range are most sensitive to climate variables which cause recognizable variation in ring widths needed for cross dating sample specimens (Abrams et al., 1998; Luckman, 2007). This sensitivity to climate variables is complex due to species specific drought adaptations (Abrams et al., 1998). Two studies have been conducted analyzing tree ring dating in conjunction with analyzing the chronology for an environmental signal (dendroclimatology) to reconstruct past climate in the Texas Hill Country, using Post oak (*Quercus stellata*) (Cleaveland, 2006) and Bald cypress (*Taxodium distichum*) (Cleaveland et al., 2011), both deciduous trees.

The dominant canopy forming species at the research site are Plateau live oak (*Quercus fusiformis*) and Ashe juniper (*Juniperus ashei*), both evergreen trees. These are less than ideal trees for dendroclimatological analyses due to their evergreen growth habit, their general location in sub-tropical latitudes, and their specific location in a heavily wooded area with intense competition for light, as evidenced by self-pruning. These characteristics cause ring boundaries to be obscured which interferes with accurate dating needed for dendrochronology and the isolation of the environmental signal needed for cross-dating and for climate reconstruction in dendroclimatology. Bartens et al. (2012) noted the difficulty of obscured ring boundaries in Live oak (*Quercus virginiana*), a closely related species to the Plateau live oak. While this study used some of the same techniques as dendroclimatology, the main goal of using these

techniques was to describe how carbon sequestration has changed over time in the system.

The research objectives were to 1) use sampling techniques to establish absolute canopy tree density and relative species density; 2) use biometric techniques to establish current biomass; and, 3) use dendrochronology techniques to determine ages and biomass history.

## **Methods**

### *Sampling plan*

A site was chosen in a closed canopy wooded area within the sampling footprint of an eddy-covariance tower in the Ameriflux network (US-FR3). Two steel cables, each of 75 meters length, were erected as a 150 meter line transect cutting across the long axis of the eddy covariance flux footprint. The transect was interrupted in its center by a rarely used, unimproved road, approximately 6 m wide that was oriented perpendicularly to the transect. A nearest-neighbor (NN) sampling plan was performed by measuring the distance from points selected on the transect to the nearest tree meeting certain criteria described below. This technique is performed in a manner similar to “distance sampling” techniques, but does not have the critical detection function required to be a distance sampling technique (Buckland et al., 1993). It is instead a variable-radius-point-quadrat sampling technique. Buckland et al. (1993) and Diggle (2003) only recommend this method for estimating tree densities in forest stands and recommend the practice of using a systematic sampling plan, but being vigilant that transects run across a disturbance or geographic gradient rather than along it. Following

these guidelines, marks were placed systematically along the transect cable every 10 meters to serve as sampling points and the 2 center transect endpoints closest to the road were excluded as sampling points to provide a 10 meter buffer to any disturbance caused by the road.

Criteria were developed prior to sampling to prevent on-site biases from influencing the selection. The trees selected for sampling were those which were closest to the respective sampling mark on the line-transect possessing the following characteristics:

- 1) They had to be of the correct species (juniper for one dataset and oak for the other dataset).
- 2) They had a substantial crown in the canopy that was exposed to the sun between 1000 and 1400 hours.
- 3) Their trunks were substantially vertical, arbitrarily field-defined as not leaning more than 25 degrees from vertical.
- 4) They were healthy when visually compared with other trees in the canopy.
- 5) Multi-trunked trees contributing to the canopy were rare and treated as a single tree, but the leaning criterion described in number 3 above was modified to allow for the trunk bending into the common base.

#### *Field measurements*

Measurements were made from the transect sampling mark to each of the selected trees to the nearest 0.01 m. Tree height was measured using a Haglöf electronic clinometer (Haglöf corp, Långsele, Sweden) The selected trees' diameter at 137 cm

(the forestry standard height for dbh or diameter at breast height) above ground level was measured with a forester's tape measure (Spencer Products Co., Seattle, WA, USA). The distance to and species identification of other canopy trees encircling and whose branches interlocked with the selected trees were recorded. The count and species of all understory trees within the radii of the canopy tree circles were recorded. Selected trees were cut at ground level. For a subsample, total above-ground wet weight was measured using a cattle scale. It was not possible to transport oaks with a dbh greater than 30 cm to the scale and therefore these measurements were biased toward the smaller oaks in subsequent biometric calculations. Also for a subsample, leaves were manually pulled off the branches of entire trees and weighed while wet and then dried in an oven at 105C and weighed again. For each tree which had its above ground biomass weighed *in toto*, cross-sectional 10 cm thick subsamples cut from the trunk were weighed while wet and then dried in an oven at 105C and weighed again.

#### *Density calculations*

Trunk density ( $\widehat{D}$ ) was calculated independently for juniper ( $\widehat{D}_J$ ) and for oak ( $\widehat{D}_O$ ) using the nearest neighbor method given by Buckland et al. (1993) which is shown here with descriptions specific to this study:

$$\widehat{D} = \frac{kn}{\pi \sum_{j=1}^k \sum_{i=1}^n r_{ij}^2} \quad [2.1]$$

where  $k$  is the number of oaks, junipers or canopy trees measured,  $n$  is the number of distances measured to each oak, juniper or canopy tree, and  $r_{ij}$  is the distance in meters of the  $i^{\text{th}}$  nearest oak, juniper or canopy tree to the  $j^{\text{th}}$  sampling point on the transect where  $i=1, \dots, n; j=1, \dots, k$ . This resulted in units of  $\text{m}^{-2}$ . To convert to  $\text{ha}^{-1}$ ,  $\widehat{D}$  was multiplied by 10,000.

Equation 1 is the general form for the group of sampling techniques known as nearest neighbor including more complex variations which measure multiple trees at each location ( $n>1$ ). The equation can be simplified for this study because only one tree of each species was selected at each location ( $n=1$ ):

$$\widehat{D} = \frac{k}{\pi \sum_{j=1}^k r_j^2} \quad [2.2]$$

Although the above equations give an estimate of the density for the species being considered, they provide no indication of possible error or variation. For that, Hedley and Buckland (2004) recommend using jackknife or bootstrap resampling techniques. In the jackknife method, a sample is dropped from the sample set and the statistic, in this case density, is calculated to obtain an  $n-1$  estimate of the statistic. The first sample is replaced in the sample set and the second sample is dropped from the sample set to obtain a second  $n-1$  estimate. This procedure is repeated until all samples have been dropped from the calculation once. This produces a range of  $n$ -values (density values in this case) from which a mean and a standard deviation of the values can be calculated. The jackknife method is deterministic and will produce the same results each time it is calculated on the same samples.

The bootstrap method relies on a random reselection of the samples with replacement after each selection, resulting in the same sample potentially being selected multiple times in each bootstrap iteration. As an example, if original samples were 1, 2, 3, 4, 5, 6, 7, 8, 9; then it is intuitively known and easily calculated that the average is 5. A 10 iteration bootstrap resampling is presented in Table 2.1. Averaging the bootstrap averages out to 1000 iterations shows that it approximates the value of 5 (Fig. 2.1). The standard deviation of the bootstrap averages as a function of the number of iterations is also shown (Fig. 2.1). The standard deviation of the bootstrap averages is the standard error of the estimate of the population average. This is referred to as the standard error of the mean (SEM). Therefore, the statistical estimate of the example population average is  $4.98 \pm 0.93$ . This will change slightly each time that the bootstrap procedure is performed because bootstrap is not deterministic.

**Table 2.1 Example of bootstrap operation.**

Samples	Average
32998158	5.625
21823119	3.375
34622337	3.75
75674296	5.75
12365737	4.25
91815443	4.375
99969459	7.5
28147993	5.375
82354676	5.125
45878633	5.5
Average	5.0625

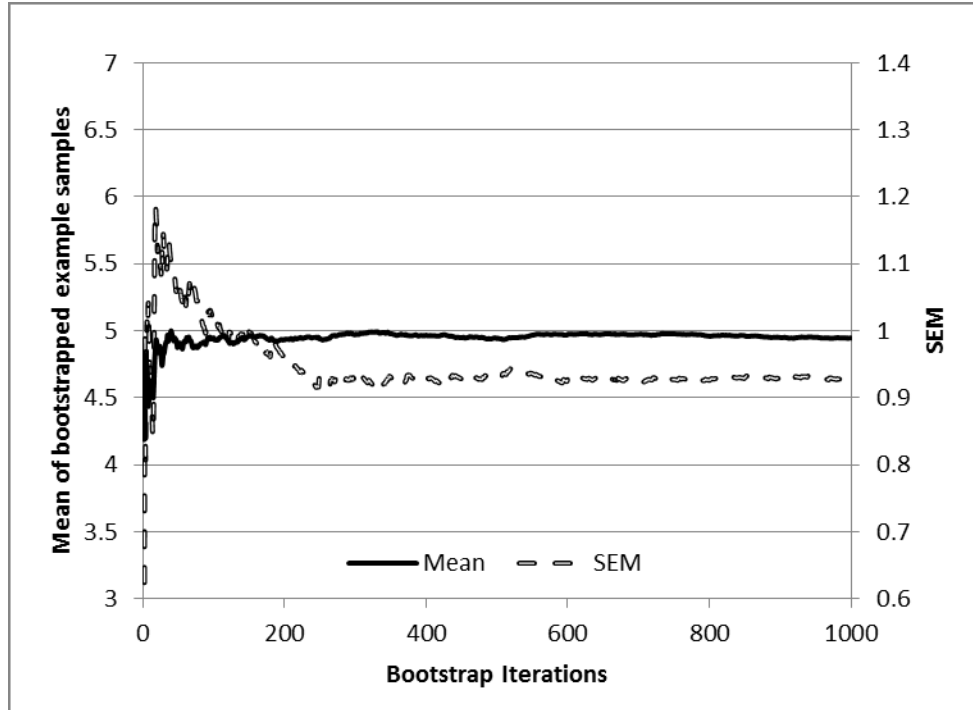


**Fig. 2.1** Example bootstrap procedure carried out to 1000 iterations.

Jackknife is not recommended for small sample sizes and therefore a 10,000 iteration bootstrap resampling (with replacement) operation was performed for each species, giving 10,000 bootstrap estimates each of  $(\widehat{D}_j)$  and  $(\widehat{D}_o)$ . Mean  $(\widehat{D})$  and standard error were then calculated for each species from the bootstrap estimates.

Density calculations using the NN formula on regularly spaced sampling points produce an inaccurate estimate of population density for species which do not have a random spatial distribution. In particular, density for species exhibiting a cluster pattern is underestimated by this technique. Plateau live oak are known for forming mottes,

clusters of trees which appear to be a single large tree when viewed from a distance (Knight et al., 1984). Although no mottes were identifiable in the heavily wooded area of study area, remnants of past mottes may contribute to a non-random distribution of the oak trees sampled in the study. A variation of nearest neighbor method (NN2) uses a search area centered on a line-transect sampling point to locate the first nearest neighbor specimen just as in the NN method, but then uses the location of the first nearest neighbor as the new center of the search area to find the second nearest neighbor. The distance between the first and second nearest neighbors then becomes  $r_{ij}$  in equation 2.1 or  $r_j$  in the equation 2.2. This method is meant to overcome errors associated with evenly spaced distributions, but overestimates density with clustered distributions. Both NN and NN2 were performed on the dataset. If the results of the two methods differ substantially, then a clustered distribution may be assumed.

#### *Dendrochronology of juniper*

The dried cross-sectional samples were sanded on a horizontal belt sander with progressively finer grits beginning with 60 and ending with 200. They were then sanded using a hand-held belt sander with progressively finer grits starting at 200 and ending with 800. Rings were measured on a Velmex measuring stage (Velmex Inc., Bloomfield, New York, USA) to the nearest 0.001 mm on three different radials from the pith to the edge. The optimal time for harvesting trees for dendrochronological analysis is in the fall. However, the time available for the work was in mid-summer 2012 and 2013. This resulted in the last ring being a partial ring and ill-defined. Therefore, the primary marker years were defined as the 2007-2008 couplet because

2007 was a very high precipitation year while 2008 was an extremely low precipitation year, resulting in a distinctive pattern. In juniper, this pattern was evident in all samples. The readings were processed for statistical analysis using Excel (Microsoft Corp, Redmond, Wa), Tricycle and Cofecha (<http://web.utk.edu/~grissino/software.htm>).

### *Dendrochronology of oak*

The oak samples were processed identically to the juniper samples. They were also cut during the summer which resulted in the last ring being partial and ill-defined. However, unlike juniper, the 2007-2008 couplet could not usually be identified and date assignments were uncertain. This was not the case in an unpublished preliminary study conducted to determine the suitability of this species for dendrochronology studies. In that study, exact dating of rings could be ascertained using the 2007-2008 couplet as the primary marker set. However, the preliminary study was conducted outside the main study area in locations with varying tree density. The clearest readings came from lone trees and trees growing in isolated mottes. Trees growing in the main study area exhibited much smaller rings, unclear ring porosity and much higher levels of heartwood discoloration, both in amount of darkening and as a percentage of cross-section. These characteristics greatly impeded identification of annual rings in the samples. Accurate dating is a cornerstone assumption of dendrochronology and especially for correlation studies in dendroclimatology. Therefore, significant efforts were made to resolve the conflicting dates, including visual re-examination of the samples, use of a variety of spline stiffness values in processing ring width values with Cofecha, sequentially analyzing each ring-width series against a master series in Cofecha as if it were undated

and by setting an annual precipitation index as the master-series against which all tree ring series were compared. Despite this, neither the age of any oak nor its growth rings dated. However, two to four rings on each tree could be traced around the entire circumference of the sample and the corresponding values for readings on each of the radials found to give a quantifiable measurement of the error. Although a correct date for these marker rings was not known, the average of the readings gave a best available estimate of the date and the differences between the three readings and the average used to calculate a percent error of the readings.

#### *Biomass calculations*

Due to the difficulty in exactly dating the oak annual rings, rather than attempt to create a master series model, the average of the three radial measurements on each tree was used to calculate biomass history on a per-tree basis and the results summed and extrapolated to a per-hectare basis. The junipers were able to be dated and a master series created, however to be consistent with the treatment of the oaks, the average of the radial measurements of each tree were used for calculating a biomass history of that tree and the results extrapolated to a per hectare basis. For both juniper and oak, some samples were excluded from the analysis due to poor readability.

For calculating biomass, the equation of Jenkins et al. (2003) was used:

$$bm = \text{Exp}(\beta_0 + \beta_1 \ln(dbh)) \quad [2.3]$$

where  $bm$  is the total aboveground biomass (kg, dry) for trees  $\geq 2.5$  cm dbh, and  $dbh$  is the sample tree's diameter (cm) at 137 cm above ground level.  $\beta_0$  and  $\beta_1$  were estimated

by linear regression analysis of  $\ln(\text{bm})$  versus  $\ln(\text{dbh})$  for a subsample of the trees which were harvested ( $n=10$  for juniper and  $n=6$  for oak). The four largest oak samples were too large to transport to the scale. Consequently, their biomass had to be estimated by application of the equation above and estimates of  $\beta_0$  and  $\beta_1$  developed using the remaining 6 measured weights.

To generate a biomass history for each tree, the average of the tree ring widths for that year was removed from the radius for one year at a time and the biomass recalculated. An assumption of this method was that all variation in diameter was due to the addition of annual rings in the xylem of the tree. A corollary to this is that the bark thickness was unchanged and this was clearly not the case when analyzing back to very young ages. However, this study primarily addressed carbon and water dynamics in canopy trees and biomass errors for when the trees were seedlings was ignored.

## **Results**

### *Tree density*

The measurements taken for calculating tree density are shown in Table 2.2. The NN estimates for canopy juniper and oak density were  $184 \text{ ha}^{-1}$  and  $55 \text{ ha}^{-1}$ , respectively. Bootstrapping altered the estimates to  $202 \text{ ha}^{-1}$  for juniper and  $71 \text{ ha}^{-1}$  for oak. The measurements of the NN2 method are shown as well in Table 2.2. The NN2 method

estimates for canopy juniper and oak density were  $668 \text{ ha}^{-1}$  and  $312 \text{ ha}^{-1}$ , respectively. The bootstrapping procedure altered these estimates to  $713 \text{ ha}^{-1}$  for juniper and  $394 \text{ ha}^{-1}$  for oak. The large difference between the species-specific NN and NN2 estimates suggests that the distribution was non-random. Neither method can be used to calculate a density for a clustered distribution which might be assumed by the tendency of this species of oak to form mottes, but NN2 can be used for estimating the density of even distributions. The even distribution in this case was the spacing of canopy-forming trees without regard for their membership in a specific species. They can be treated as a single group because the p-value in a two-tailed, two sample t-test is 0.42, indicating that distance measurements of the oak and juniper were not significantly different at the  $\alpha=.05$  level. Therefore, the NN2 method was performed on the pooled measurements as shown in Table 2.3. In the previous instance of NN2, the sample population was restricted to the distance between same species 1<sup>st</sup> and 2<sup>nd</sup> nearest neighbors. However, in the pooled instance, both same species and different species were viable contenders for being 1<sup>st</sup> and 2<sup>nd</sup> nearest neighbors, making the two datasets somewhat different.

**Table 2.2 Data and results for the two variations of the nearest neighbor estimates (NN and NN2) using species-specific data.**

Method	NN		NN2	
	$R_{ij}$ (m) for oak (k=10)	$R_{ij}$ (m) for juniper (k=10)	$R_{ij}$ (m) for oak (k=9)	$R_{ij}$ (m) for juniper (k=10)
Measurements	5.53	1.85	2	1.7
	4.42	3.1	1.21	1.1
	3.2	5.7	1.8	3.83
	9.35	3.58	2.37	2.6
	17.5	3.4	1.35	1.3
	2.55	5.3	5.35	2.41
	1.53	0.01	0.82	0.9
	4.11	2.1	6.3	2.44
	5.9	4.16	2.55	1.96
	8.02	7.3		2
Direct estimate of $(\hat{D})$	55 ha <sup>-1</sup>	184 ha <sup>-1</sup>	312 ha <sup>-1</sup>	668 ha <sup>-1</sup>
Bootstrap estimate of $(\hat{D})$ and SEM	71 ±40 ha <sup>-1</sup>	202 ±66 ha <sup>-1</sup>	394 ±243 ha <sup>-1</sup>	713 ±195 ha <sup>-1</sup>

**Table 2.3 Data and results for the NN2 calculation of density using pooled data and assuming a non-random but even distribution of trees.**

Method	NN2 (pooled)			
	$R_{ij}$ (m) any species (n=1) (k=20)			
Measurements	1.7	2.41	2	2.83
	1.1	0.9	0.36	0.82
	3.83	0.47	1.8	2.91
	2.6	1.96	2.25	2.55
	1.3	2	1.35	1.47
Direct estimate of $(\hat{D})$	777 ha <sup>-1</sup>			
Bootstrap estimate of $(\hat{D})$ and SEM	807 ±160 ha <sup>-1</sup>			

The estimate of 807 trees ha<sup>-1</sup> can be partitioned by species using the survey of canopy species performed at each first nearest neighbor prior to harvesting it. The results of that survey are in Table 2.4.

**Table 2.4 Partitioning tree density into species density.**

Species	count	Percentage	Density
elm	3	4	32 ha <sup>-1</sup>
juniper	41	49	395 ha <sup>-1</sup>
oak	39	47	379 ha <sup>-1</sup>

### *Dendrochronology*

Age of junipers ranged from 20 to 60 years old (Fig. 2.2). High precipitation years were easy to recognize because the junipers formed light rings in the growth between the dark annual rings during these years. The light rings appeared to be the result of exuberant growth directly after large rainfall events. Juniper expressed no evidence of decreasing radial growth with age (Fig. 2.3) such as would be expected if the trees were approaching the maximum age for the species or if competition were increasing.

The dating of the oak cross sections was more difficult. There were very few clues with regard to the climate and weather, but each tree exhibited 2 or more years of very clear and distinctive growth which could be traced around the circumference of the tree. These full-circumference distinctive rings did not correspond between trees and therefore appear to be responses to events unique to the individual tree. An absolute

deviation for the radial readings of these unique events was calculated as the absolute value of the difference between the average of the radial readings and each radial reading. The average absolute deviation for all unique events was 0.69 years. This was normalized over the number of years prior to harvest that the event took place, resulting in 0.029 years of deviation per year before harvest or  $\pm 2.9\%$ , which was used as the error term in the age calculations for oak. Like the juniper, oak exhibited no decrease in radial growth with age (Fig. 2.3).

#### *Biomass calculations*

Regression analysis was used to obtain slope and intercepts for the Jenkins et al. (2003) model (Eq. 2.3) as shown in Fig. 2.4. Equation 2.3 was then used to reconstruct the individual biomass histories of all study trees (Fig. 2.5). Despite the slightly higher density of juniper, oak dominated the above-ground standing biomass on a dry-weight basis at  $108 \text{ Mg ha}^{-1}$  as compared with  $18 \text{ Mg ha}^{-1}$  of juniper (Fig. 2.6). From 1992 to 2012, oak exhibited approximately 4 times the annual biomass gain per hectare of juniper. This was largely due to the oaks being older than the juniper and having larger diameter and height. Junipers are increasing their share of the total biomass at an annual rate of 0.22% (Fig. 2.6).

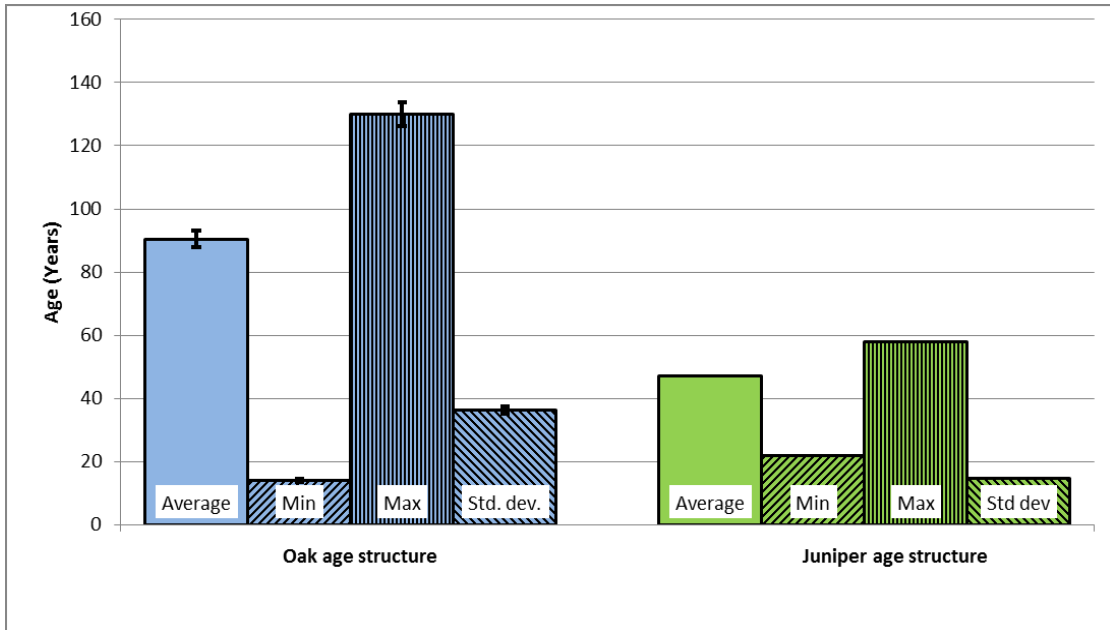


**Fig. 2.2** Age structure of the two dominant canopy species. Error bars on the oak statistics represent average relative deviation, which is 2.9% of the age estimate.

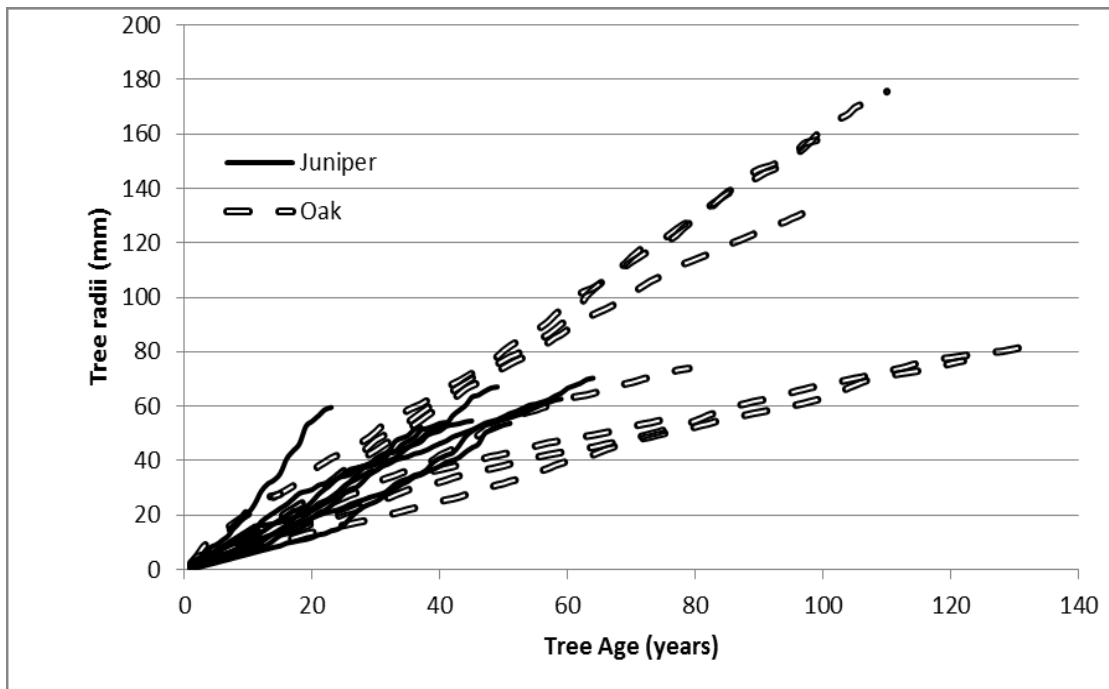


**Fig. 2.3** Tree radii history at dbh.

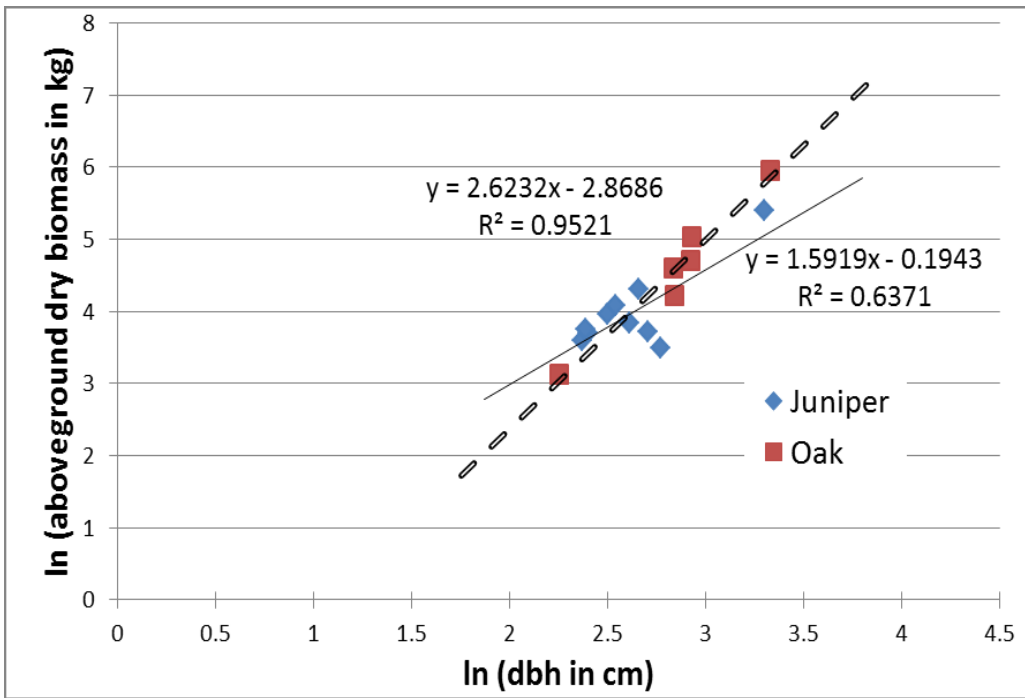


Fig. 2.4 Biomass plots to estimate parameters for equations by Jenkins et al. (2003)



Fig. 2.5 Biomass history of the study trees.

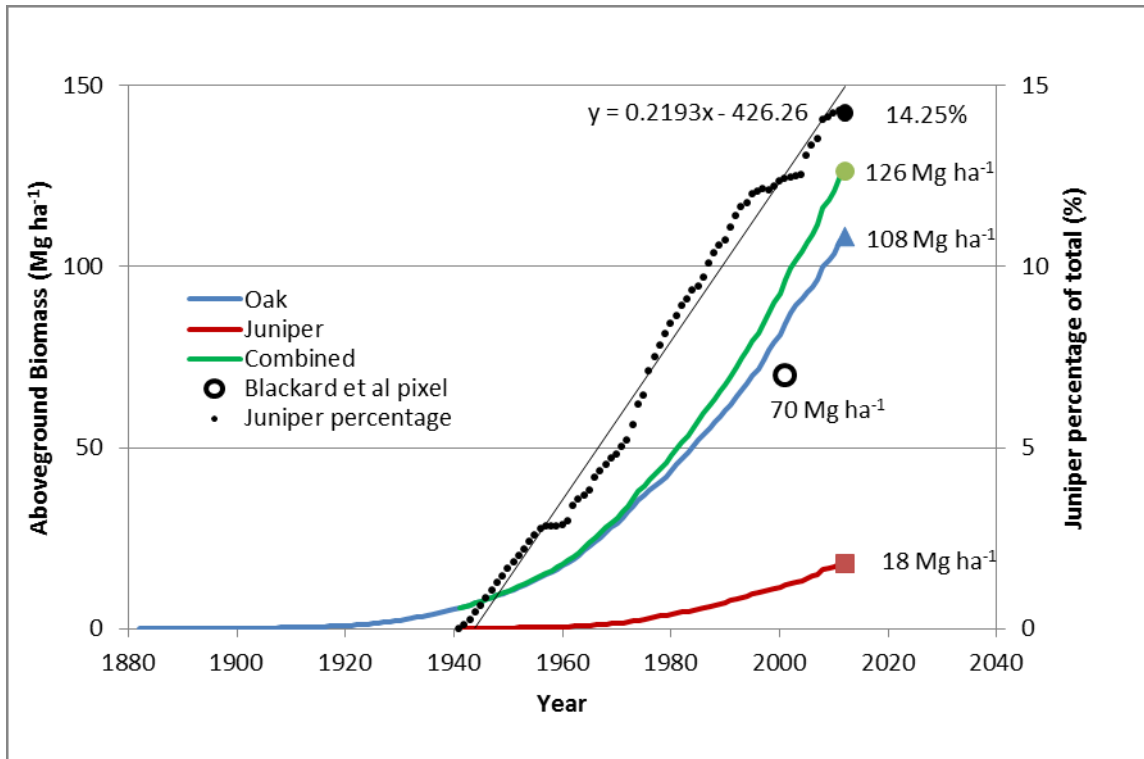


Fig. 2.6 Biomass history extrapolated to a per hectare basis.

## Discussion

The forest around the eddy covariance tower at Freeman Ranch is fairly young and is a first growth as a closed canopy forest rather than scattered trees in a savanna. The maximum oak age in the study was 130 years in contrast with the study by Bartens et al. (2012) where the average age of a closely related species in their study was 175 years, and referenced anecdotal evidence of 500 year old trees. Larger diameter specimens of both oak and juniper were evident on Freeman Ranch by casual observation and oak mottes are a regular feature on the ranch. The mottes are indicative of a potentially longer history than any of the individual trees composing the motte

unless the founding tree still lives, usually located in the center of the motte and possessing a much larger diameter trunk (Barnes et al., 2008). These scattered large diameter and presumably very old trees of both species likely provided the seed source for the present dense forest. Fire suppression in the modern era is frequently cited as the reason for the expansion of juniper from draws and rocky outcrops into dense thickets because juniper readily burns and does not resprout from the root crown (Auken and Smeins, 2008; Barnes et al., 2008; Wink and Wright, 1973). For this reason, juniper is seen as a native-invasive expanding into the niche normally occupied by oak. Oak is moderately fire resistant and will resprout from the root crown if it does burn, even producing a crop of acorns within 5 years of resprouting. However, in this study, individuals of both species are relatively young compared to their potential and neither is exhibiting a decrease in radial increment expected due to age-effect or competition. If this is evidence of juniper invading savannas, then it is also evidence of oak invading savannas to a much greater extent than was historically supported by the ecosystem (Russell and Fowler, 1999). Both species appear to be native-invasives expanding their niche. Ansley and Rasmussen (2005) state that a fire frequency of 6 years or less is necessary for juniper control in the Great Plains. In a nearby area of Freeman Ranch, a 2 hectare crown fire in 2000 caused an opening in the canopy where grass once again dominates. This fire was not allowed to burn to its natural completion and the resulting clearing was only a small portion of the woodland. Within the burned area, juniper and oak seedlings have sprouted and many oaks have resprouted from their root crown. However, a heavy grass fuel load and the relatively low height of the young trees means

that they are more susceptible to fire damage (Wink and Wright, 1973) if fire were not actively suppressed. If a fire frequency of 6 years is required for juniper control, then the clearing is past due to burn again.

Using 2001 MODIS images, Blackard et al. (2008) produced a map of biomass for the continental United States of sufficient resolution that the pixels of the heavily forested study area could be roughly identified. Estimated biomass for this pixel,  $70 \text{ Mg ha}^{-1}$ , compared with the  $92 \text{ Mg ha}^{-1}$  in 2001 found in this study (Fig 2.6).

Although the average age difference between the two species is well described in this study, it is not well explained by fire suppression since, presumably, the beginning of fire suppression which aided the oak to expand their niche would simultaneously have aided the juniper, resulting in an even aged stand of the two species. To explain the age differences, differential herbivory, successional changes and dispersal mechanisms need to be examined. Specifically, live oak acorns and seedlings are highly palatable to white tail deer, while juniper are not. Deer were hunted to the point of near extinction in the late 1800s statewide until effective hunting regulations and restocking programs brought them back into abundance in the early 1900s. Between these years, live oak had the opportunity to establish in grasslands. Junipers are spread by birds and are not shade tolerant (Auken and McKinley, 2008). It may be that when oaks became established to a certain size and started a nascent motte, they provided a habitat for birds which then passed the juniper seeds through their digestive tract in a circle around the trees. Those seeds which fell inside the tree canopy footprint failed to establish or thrive while those falling on the edge or outside the tree or nascent motte became established. Juniper

seedlings are thought to benefit greatly from a nurse plant for initial survival, but low growth rates are found in the most shaded area under the nurse plant and high growth rates are found on the edges (Auken and McKinley, 2008; Barnes et al., 2008; Owens, 2008). This nascent motte of the oaks and inverse motte of the junipers could account for the clustered distribution found in the species-specific NN and NN2 calculations of density.

Juniper respond to annual rainfall by varying the width of their annual radial ring width increment enough to use dendroclimatological techniques for cross-dating. Since they form both false rings (dark rings which can be mistaken for annual rings) during dry periods as well as light colored rings apparently as a growth response to large rainfall events, it may be possible to use this species for a finer temporal scale dendroclimatology study with more development of techniques. These sub-annual features of the juniper demonstrate that they are actively growing radially most of the year. Conversely, oak radial growth increment does not vary with annual precipitation and no sub-annual features could be discerned. During the microscopic examination of the oak rings, some cross sections exhibited what could have been a response to annual precipitation in 1957, 2004 and 2007, but the difficulty in precisely dating these cross sections made it difficult to ascertain with any degree of certainty. This could mean that the oaks are not growing on the edge of their range, that they have a different carbon storage and allocation system, or that rain is not the most limiting factor for this species. It is especially perplexing given that cross dating for this species was much easier for oaks growing in the open or in an isolated motte.

## **Conclusions**

Oaks and juniper are locked in competition at Freeman Ranch with no clear “winner” and “loser.” Both are expanding their niche into the grassland part of the savanna creating a forest in its place. The oak have an advantage of being established at an earlier date while juniper are growing and reproducing faster. This results in a clear dominance for oak in terms of carbon sequestration currently, but juniper are gaining yearly as a percentage of the total. Fire and fire suppression are wildcards in the competition. Oak is much more adapted to fire than juniper and a crown fire could reset the balance for decades, first to grasses but gradually to oaks and then back to a competition between oak and juniper. Absent fire, it seems likely that the juniper will become self-limiting due to its intolerance for shade. Oak’s tolerance for shade likely means that it will never be completely eradicated from the landscape by juniper.

Many questions remain and still more suggested by this study. A comprehensive study of the 2 hectares burned in 2000 to determine survival, growth rates and carbon dynamics is needed for a comparison with the present study. The study by Bartens et al. (2012) included 137 samples, giving them ample buffer for throwing out problematic samples. The present study had far fewer and little leeway to throw out problematic samples. Dispersal mechanisms to explain differences in average age deserves a more focused investigation.

CHAPTER III  
EMPIRICAL CALCULATION OF THE WATER YEAR IN SUB-TROPICAL, SEMI-  
ARID FORESTS

**Introduction**

Two different annual timeframes are in use for reporting annual rainfall, the calendar year, running from January 1 to December 31, and the USGS water year, running from October 1 to September 30. In the Pacific northwest prior to the development of the USGS water year, the annual calendar year input (precipitation) and outputs (runoff, percolation to groundwater and evapotranspiration (ET)) of water in the ecosystem did not balance because of a large amount of water storage (S) in the form of snow already present at the beginning of the calendar year. Also, there was a large amount of S at the end of the calendar year from snowfall in the last quarter. The change in water storage ( $\Delta S$ ) between the beginning and end of the year had to be included in order to balance the water budget,

$$W_{in} = W_{out} + \Delta S \quad [3.1]$$

where  $W_{out}$  is the annual output of water from the system including runoff, recharge to an aquifer and ET, and  $W_{in}$  is annual precipitation. In the nomenclature of Huang and Wilcox (2005) working on the Edwards Plateau, this can be expanded to,

$$P = (Q + R + ET) + \Delta S \quad [3.2]$$

where Q is surface runoff, R is recharge to an aquifer and P is precipitation.

The USGS water year starting October 1st was introduced a century ago as a logical accounting method to have snowfall from the end of one year carry forward until the snow melts the following spring (Henshaw et al., 1915) when it can be used by plants, recharge aquifers or run off in streams. By doing this, interannual  $\Delta S$  is minimized (Follansbee, 1994; van Lanen et al., 2004) and correlation between  $W_{out}$  and  $W_{in}$  is maximized.

This water accounting timeframe has been generally applied across the United States by the USGS (Follansbee, 1994; USGS, 2013) and is used by some researchers (Steinwand et al., 2006) although the calendar year continues to be used by other researchers (Scott, 2010; Scott et al., 2004). Other water-year start dates have been used by other organizations and researchers for water accounting purposes including dates in June, July, September and November (Falk et al., 2008; van Lanen et al., 2004). Additional water year start dates have been defined for other purposes such as April 1st for defining a “low-flow” year (USEPA, 2013) and May 1st for optimal synchronization of two adjacent watersheds (Inaba et al., 2007). In this study, I ask if the USGS water year is the most appropriate annual timeframe for water accounting in a semi-arid, subtropical climate which is highly disparate from the Pacific Northwest climate that gave rise to the USGS water year. This is done by testing not just January 1<sup>st</sup> and October 1<sup>st</sup>, but all 365 possible days (ignoring leap days).

The test site is a semi-arid, subtropical, forested environment in the Texas, USA “Hill Country” along the eastern margin of the Edwards Plateau. The site is equipped with an eddy flux tower on a jointed limestone outcrop. The limestone outcropping

makes it difficult to directly measure water storage at this site. However, rather than attempting to measure annual  $\Delta S$ , an annual timeframe was developed in which the interannual variation in precipitation maximally explains the interannual variation in the outputs.

Evapotranspiration is the fate of the majority of precipitation at this site, accounting for 76% to 92% of annual precipitation in previous studies (Heilman et al., 2014; Heilman et al., 2009). The only storage occurs within the soil and dissolution cavities since temperatures are too high for storage as snow. Of the outputs, ET is the only output from storage. Runoff doesn't make it into storage and recharge can be considered passing through storage quantitatively (Afinowicz et al., 2005) although qualitatively there may be a displacement effect causing new water to enter storage and old water to be contributed to recharge (Jones, 2013). Therefore, the criterion for this study will be to select a start date for an annual timeframe in which interannual variation in P maximally explains the interannual variation in ET.

## **Methods**

### *Site description*

The study site is a closed canopy wooded area on Freeman Ranch, a 1700 ha research area near San Marcos, Texas managed by Texas State University—San Marcos. The area is a rocky outcrop of heavily jointed Cretaceous limestone. Soil is shallow in general at about 20 cm (Heilman et al., 2009), but may accumulate to a large degree in the joints and dissolution voids in the karstic landscape. Mean annual rainfall is approximately 860 mm. Annual rainfall during the study period ranged from 319 mm in

2011 to 1740 mm in 2007, using the USGS water year definition. The mean annual temperature is approximately 20°C. There are few days when the temperature does not rise above freezing and consequently there is no accumulation of snow to melt in the spring. Ashe juniper (*Juniperus ashei*) and Plateau live oak (*Quercus fusiformis*) dominate the closed, interlocking canopy at approximately 8 meters height above the ground. The canopy is composed of approximately 50% juniper and 50% oak. Cedar elm (*Ulmus crassifolia*) is present in the canopy as well, but not represented in the sampling and visually estimated to be less than 5% of the canopy. Juniper dominates the understory species at 76%, followed by oak (4%), elm (2%) and the balance to non-canopy perennial species.

#### *Precipitation and flux measurements*

Precipitation data from an on-site tipping bucket raingauge (Texas Electronics, Inc., Dallas, TX, USA) were collected for calendar years 2004(4<sup>th</sup> quarter only) to 2012. There were data gaps due to power failures that were filled manually from data collected at nearby research sites. Eddy covariance data were collected using a 3-D sonic anemometer (model CSAT3, Campbell Scientific Inc., Logan, UT) and an open-path gas analyzer (model Li-7500, LI-COR Inc., Lincoln, NE) both running at 10 Hz and mounted at 14 meters height above the ground. A prior analysis of the output of the EddyPro 3.0 program (LiCor, 2013) when processing data from this site in default configuration compared very favorably with four proprietary or in-house developed processing programs used in previous studies. However, for the sake of uniformity all raw data was processed using EddyPro 3.0 running in default mode. EddyPro version

3.0 in default configuration includes double axis wind rotation, block averaging, time lag optimization for maximum covariance, spike removal, absolute limits, WPL correction, high- and low- pass filtering, and sonic temperature correction for humidity as documented on the product webpage maintained by LiCor (2013). Flux data calculated during periods of low friction velocity (<0.15 m/s), when the instrument was in the tower windshadow, during precipitation events or when there were indications of instrument errors were rejected during post-processing, resulting in data gaps. General meteorological data collected (global radiation, relative humidity, air temperature and soil temperature) at the site was combined with the processed and filtered flux data and submitted to the online gap-filling and flux partitioning tool of Reichstein (2013) in order to obtain a continuous dataset for 8.25 years of carbon, water and energy fluxes. A combination of meteorological data, EddyPro processed fluxes, gap-filled data and partitioned data were submitted to and are available from Ameriflux as “Level 1” data. Precipitation data used in this study is unchanged from the Ameriflux “Level 1” data. However, energy balance closure was forced by partitioning the excess energy between latent heat flux and sensible heat flux while maintaining the Bowen ratio (Twine et al., 2000). Additionally, the latent heat flux values from the Ameriflux “Level 1” data are expressed as mm of ET to have directly comparable units with precipitation.

*Annual data and best fit day of year*

To find the best fit day of year, I used the function,

$$\text{Water Year Start Day} = \max_{1 \leq D \leq 365} (f(r_{(AP_D, AET_D, n)}^2, D)) \quad [3.3]$$

where the function  $f(\cdot)$  maps  $D$  to  $r^2$ , the function  $\max(f(\cdot))$  is bijective ( $D \leftrightarrow r_{max}^2$ ),  $D$  is the day of the calendar year for which the function is being evaluated,  $r_{(AP_D, ET_D, n)}^2$  is the linear coefficient of determination between annual precipitation ( $AP_D$ ) and annual ET ( $AET_D$ ) for the day being evaluated given  $n$  number of years of data, Annual precipitation in mm was calculated for a particular day as

$$AP_D = \sum_{Day=-365}^{-1} \text{Daily Precipitation} \quad [3.4]$$

and  $AET_D$  in mm was calculated for the day being evaluated as

$$AET_D = \sum_{Day=-365}^{-1} \text{Daily Evapotranspiration}. \quad [3.5]$$

Annual precipitation (mm) and annual ET (mm) were calculated for each day of all years starting in the 4th quarter of 2005. Excel 2010 64-bit edition (Microsoft Corporation, Redmond, Washington) was used for this and all subsequent calculations. For the sake of standardization, “annual precipitation” was considered to be the sum of the rainfall occurring during the previous 365 days, without regard to the 2 extra days in the study due to leap years. “Annual ET” was treated in an identical manner.

I compared the coefficient of determination ( $R^2$ ) from a linear regression analysis of annual ET with annual precipitation for January 1<sup>st</sup> and for October 1<sup>st</sup> to find the start date which gave the best fit. This same analysis was performed for each day of year (DOY) to give a complete picture of the annual variation.

### *Lag adjustment*

Optimizing the start date for a water year doesn't remove lag between AP and AET, but makes the lag relatively less consequential on annual data because the longest dry period comes at the end of the year. Very small values for the non-lagged precipitation data during the dry period do not affect the final balance much and allows the lagging ET data to catch up. However, adjusting the alignment of the data for maximum correlation removes the lag and shows the true dependency of AET on AP.

A correlation coefficient (Pearson's  $r$ ) was calculated for AP and AET starting together and then lagging AET in a 1 day step-wise manner through 365 days. The lag time with the maximum correlation was found and all ET data adjusted to form a "Lagged Annual ET" dataset.

## **Results**

### *Start date determination*

Starting the annual timeframe on the first day of the calendar year gave an  $R^2$  of 0.59 (Fig. 3.1). Then the general  $R^2$  trend decreased to 0.02 on day 149 and then increased to a maximum of 0.93 on day 274 which corresponds to October 1<sup>st</sup>, the start date of the USGS water year. A sharp drop occurred at 320 days.

### *Lagging*

Lagging can be best visualized by looking at a time series plot of annual precipitation and annual ET (Fig. 3.2). Lagging AET in a 1 day step-wise manner resulted in a smooth bell curve with a maximum correlation value of 0.893 at a lag value

of 95 days (Fig. 3.3). Lagging improved the explanatory power of annual precipitation on annual ET generally (Fig. 3.4) and specifically for the USGS water year from 0.93 to 0.97 (Fig. 3.1, day 274). The 95 day lag causes the starting data for annual ET to fall on January 4<sup>th</sup>, which closely approximates the calendar year. Note that lagging improves goodness of fit regardless of the chosen start date.

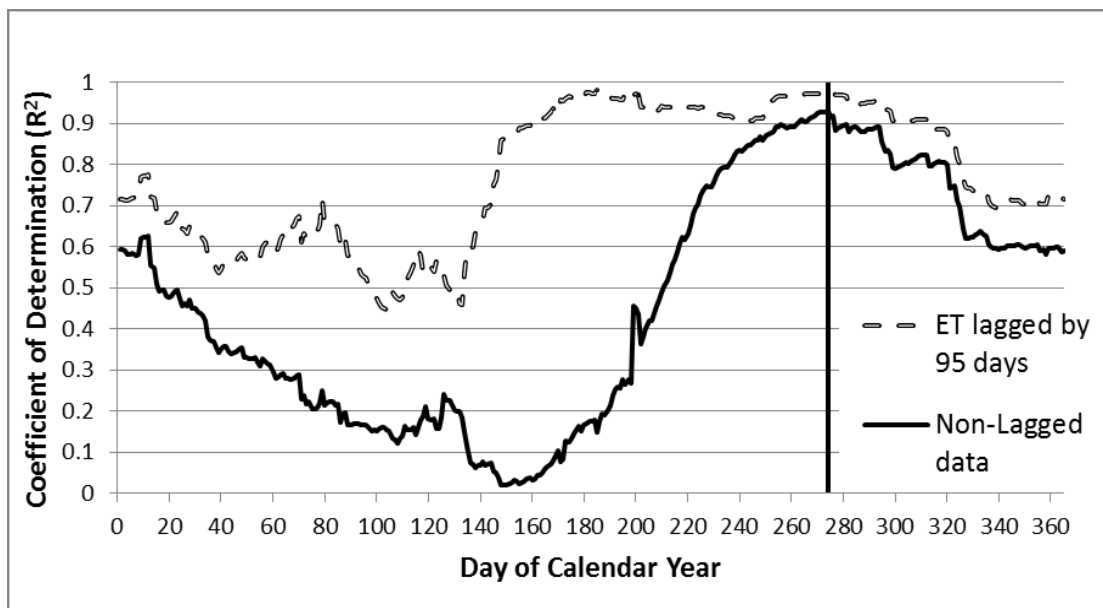


**Fig. 3.1** Coefficient of determination between AP and AET.

## Discussion

The start date for a water year that maximized correlation between inputs and outputs and minimizes  $\Delta S$  in this test ecosystem was calendar day 274. This is the same as the start date determined a century ago for the Pacific northwest ecosystem and

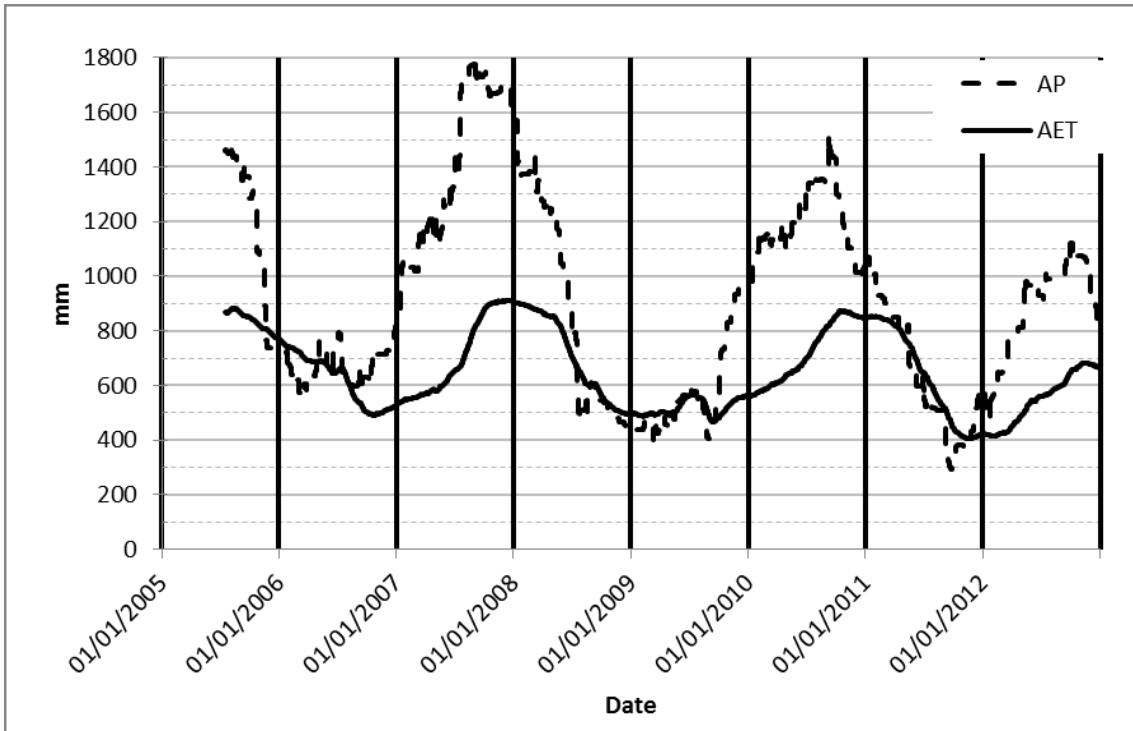


**Fig. 3.2** Graph showing the lag between AP and AET

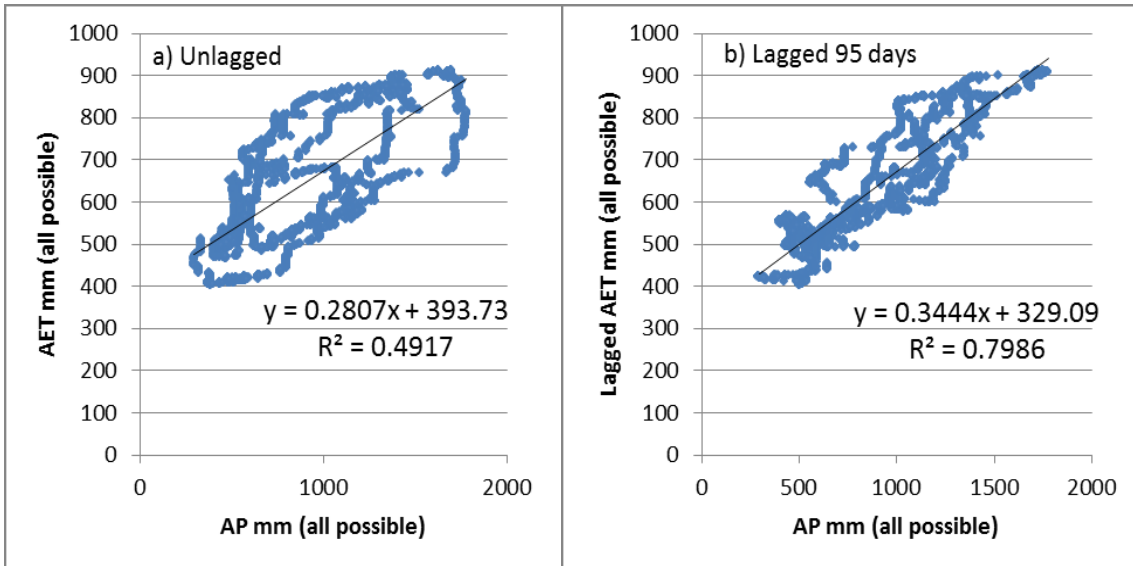


**Fig. 3.3** Improvement in goodness of fit when lagging AET by 95 days.

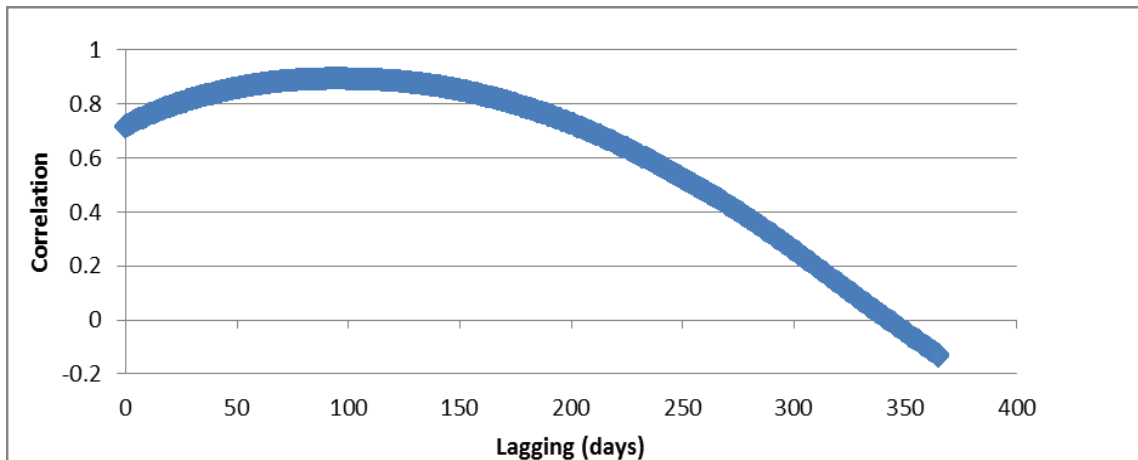


**Fig. 3.4 Correlation between annual precipitation and annual ET as a function of lag time.**

generalized across the continent by the USGS as their water year for accounting purposes. Although the methods appear to be dissimilar due to data collection protocols, the goal of the two methods is identical, to maximize correlation between inputs and outputs and to minimize  $\Delta S$ . What has changed is the form of the inputs (San Marcos has negligible snowfall) and the major outputs (ET rather than runoff). That two such disparate ecosystems had the same start date for their water year was surprising, but a similarity was expected because of similar timing of seasonal patterns of light, temperature and precipitation.

AP diverged from AET when AP was rising as seen in Fig. 3.2. However, when AP was falling and became less than 800 mm, AP and AET were tightly coupled. If these were tightly coupled throughout the year, then the correlation curve presented in Fig. 3.3 would have a sharp peak rather than the broad curve shown. Both the wet

times (over 800 mm and annual precipitation rising) and the dry times (less than 800 mm and annual precipitation falling) are included in the lag-correlation value and since the dry times are tightly coupled, the wet times must be more extremely decoupled than the 95 days presented.

The 95 day lag time is the best average lag time on an annual basis when optimized for high goodness of fit on the start date, but presents the problem of annual ET apparently responding before annual precipitation occurs if examined at other timeframes. The lag adjustment is primarily a mass-balance accounting tool for cumulative (in this case, annual) data to account for storage. The effect of the lag adjustment is almost negated when the start date is optimized. In this case, it only increased the goodness of fit on day 274 from 0.93 to 0.97. The lag adjustment increased the goodness of fit much more dramatically when change in storage is not controlled by optimal water year start day choice such as on day 150 (Fig. 3.1). Examining the same datasets with a quarterly timeframe rather than an annual timeframe resulted in a 29 day lag for optimal correlation between quarterly cumulative precipitation and quarterly cumulative ET and an  $R^2$  of 0.38. A monthly timeframe resulted in a 15-day lag for optimal correlation between monthly cumulative precipitation and monthly cumulative ET with an  $R^2$  of 0.22. A weekly timeframe resulted in a 9 day optimal lag and an  $R^2$  of 0.10.

The non-lagged data in Fig. 3.1 shows the effect on  $R^2$  of the lagging variable catching up during the low rainfall portion of the year until day 274 and then decreasing. In contrast, the lagged data in Fig. 3.1 has very high goodness of fit for nearly 6 months

out of the year. This confounds the notion of a distinct start date to the year as just about any day can be chosen as long as the  $R^2$  value is high. For this reason, the distinct start date is determined first and then the lag adjustment applied to optimize the choice, rather than adjusting for lag first and then attempting to find a distinct start date. In this ecosystem, using the USGS water year for summing annual precipitation and the calendar year for summing ET is a viable strategy. Anthoni et al. (1999) identified this practice as a possible source of error.

A phreatophytic strategy where plants have unlimited access to ground water should mean that AET is fairly independent of AP. This is clearly not the case in this study. Also, Heilman et al. (2014; 2009) found that evidence was lacking for significant water extraction from a perennially stable deep supply of water, and that ET was tightly coupled with precipitation. However, they left open the possibility that water is available months or even years after it fell as rain. The present study corroborates their hypothesized long-term storage. For the water year 2011, AET exceeded precipitation by 124 mm (Table 3.1) while the soils are only thought to have 70 mm of capacity (Heilman et al., 2009). Juniper are known to have some deep roots and to draw from deeper sources during the seasonal drought (McCole and Stern, 2007). Heilman et al. (2009) speculated that the storage may be a slow-recharge, slow-release intrinsic property of the epikarst which makes water slowly available to the plants. Alternative explanations are that it is caused by an intrinsic property of using deep roots (that the pathway from the water source to the leaves is longer) requires more energy, that the mass flow of water from roots in the deep storage zone is insufficient to sustain plant

metabolic activities at the same level as when all roots have access to water (Schwartz et al., 2013), or that cavitation may disrupt mass flow (Elkington et al., 2014).

The amount of water available for annual runoff and percolation (AR+P) can be found by subtracting AET from AP, assuming  $\Delta S$  is zero. Fig. 3.5 shows the results from graphing the relationship. There were two years when AR+P were negative. Since this is not possible, it shows a violation of the assumption that  $\Delta S$  is zero. The year 2009 was one of the years that violated the  $\Delta S=0$  assumption and the following year, 2010, was well below the regression line. It follows then that the negative value in 2009 represents a withdrawal from storage that had to be refilled in 2010 from the AR+P budget. If the deficit of 2009 is added to 2010 (Fig 3.5, open circle), the 2010 data point is pulled up to the regression line. Also, the x-intercept of 520 mm of precipitation

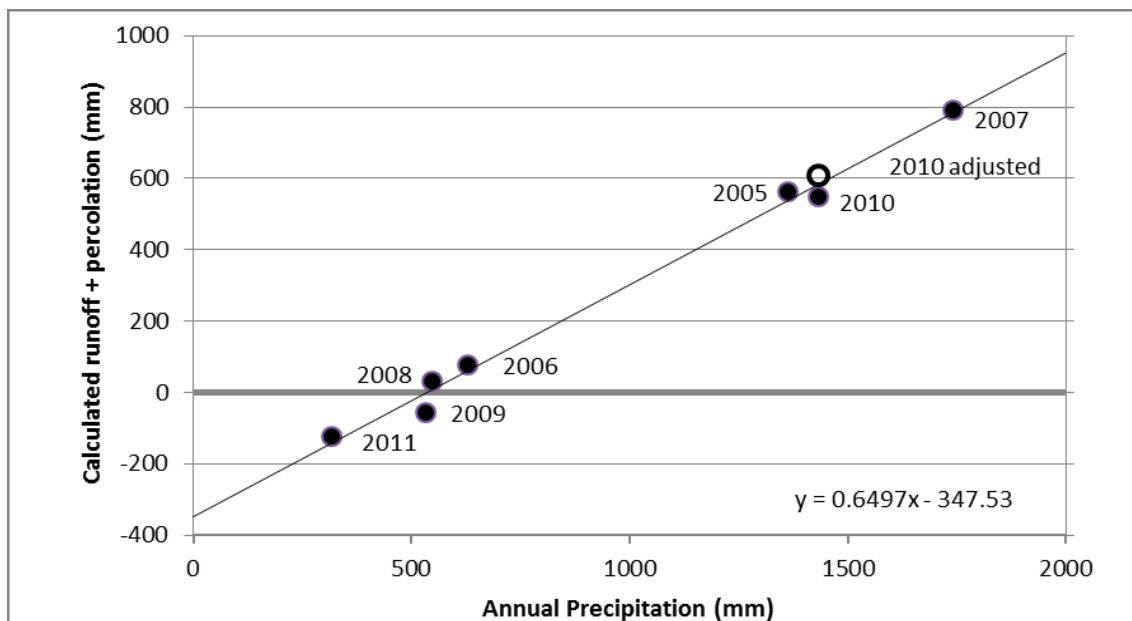


**Fig. 3.5 Runoff + percolation as a function of AP.**

appears to be a threshold that must be passed below which all precipitation ends up as ET (absent an extreme precipitation event). This agrees with the finding by Schwartz et al. (2013) that 520 mm of artificial precipitation was needed to cause an increase in dripping in caves beneath their site during the worst 1 year drought in Texas' history. It also agrees well with the 500 mm threshold of AP before any improvement in runoff or recharge can be realized with land management practices found by Wilcox (2002). The y-intercept of -347 mm represents the storage capacity of the soils and epikarst of the ecosystem.

**Table 3.1 Annualized data**

Water Year	AP	AET	AET*	AR+P	AR+P*	AET/AP	AET/AP*
2005	1363	887	800	476	563	0.65	0.59
2006	629	525	552	104	78	0.83	0.88
2007	1740	912	947	828	793	0.52	0.54
2008	547	592	516	-45	31	1.08	0.94
2009	533	503	591	30	-58	0.94	1.11
2010	1432	894	883	538	549	0.62	0.62
2011	319	466	442	-147	-124	1.46	1.39
Average	938	683	676	255	262	0.73	0.72

\* denotes the use of lag adjusted data.

## Conclusions

A general method for calculating the local water year has been presented and works well with data from the test site as measured by a strong goodness of fit to the data. In addition, the results from the test site compare exactly with the USGS water

year start date determined a century ago. This new method minimizes the change in water storage so that relationships between AP, AET and AR+P can be determined. Lag adjusting AET for maximal correlation with AP further clarifies and strengthens these relationships.

In the test ecosystem, the variation in AP has been demonstrated to explain 97% of the variation in ET with the combination of determining the best start date for the water year and lag adjusting ET data. With the very tight  $R^2$  relationships minimizing randomness in the data, anomalous data points can be rationally scrutinized and explained. Even though storage can't be measured directly, its volume can be estimated and its change can be calculated and utilized.

While the method is presented as a general method, the validity of the site calculations is limited to the area of eddy covariance footprint and substantially similar areas. Within 1 km of this site are 2 additional Ameriflux eddy covariance towers in very different ecosystems. One is a savanna with a different tree species composition, lacking a canopy, and with significant amounts of grass interwoven on comparatively deep soils. The other is a mixed C3/C4 grassland with large patches of CAM prickly pear. The method presented herein should be performed on data from these other sites to get a clearer picture of the Texas Hill Country as a whole.

## CHAPTER IV

### A GENERALIZED METHOD FOR DETERMINING A HYDRO-ECOLOGICAL YEAR AND OPTIMIZING FOR ECOSYSTEM LAG

#### **Introduction**

Plants respond to their environment in a manner which optimizes resource conversion into productivity (Agren and Franklin, 2003; Binkley et al., 2004; Bloom et al., 1985). In climates where plants are dormant in one or more seasons during the year, productivity will cycle on an annual basis in response to seasons and available resources. Seasonal changes in precipitation, temperature and solar radiation are major drivers of ecosystem productivity (Hsu et al., 2012; Rosenzweig, 1968; Urbanski et al., 2007). This seasonality should be accounted for when describing ecosystem productivity. In particular, the seasonality and inter-annual variability of precipitation bears heavily on productivity in water-limited arid and semi-arid regions (Thomas et al., 2009; Vickers et al., 2012). The seasonality of precipitation causes the balancing of a water budget to be difficult for any given calendar year as antecedent rainfall must be known to explain the water availability at the beginning of the year and then a significant balance must be carried over at the end of the year (Henshaw et al., 1915) to explain the next year's beginning water availability. An alternative to the calendar year is the "water year" developed by the United States Geologic Survey (USGS) to have an annual timeframe which balances water inputs and outputs to the maximum extent and minimize changes to storage (Follansbee, 1994; van Lanen et al., 2004). In theory, this means that each

location and, indeed, each water year would have a unique calendar start and end date. However, the start dates and end dates have been aggregately generalized to October 1<sup>st</sup> and September 30<sup>th</sup>, respectively (USGS, 2013) and this is widely used in water budget publications. Some authors define a different annual timeframe and also label it a “water year” (e.g. July to June in Falk et al. (2008)) and this necessitates more specific labeling herein to avoid confusion.

This USGS water year breakpoint may be applicable to annual productivity because plant available water is well known to have a controlling role for productivity in water-limited ecosystems. However, studies regarding productivity routinely utilize the calendar year (Afinowicz et al., 2005; Ehman et al., 2002; Heilman et al., 2014; Heilman et al., 2009; Hussain et al., 2011; Kjelgaard et al., 2008) without rigorous consideration of the alternatives. While the USGS water year facilitates water accounting in temperate North America, neither it nor the calendar year are optimal for all research questions. For instance, they are both sub-optimal for research involving the effects of low-flows on aquatic species and therefore a different purpose-defined “low flow year” starts April 1<sup>st</sup> and ends March 31<sup>st</sup> (USEPA, 2013). Inaba et al. (2007) calculated a water year to start May 1<sup>st</sup> for optimal synchronization of two watershed discharge curves. Dates in June, July, September and November have also been used to start annual timeframes, responding to the needs of the research being conducted. (Falk et al., 2008; van Lanen et al., 2004) Many use the “growing season” when discussing water-use-efficiency in plants and this is typically 3-9 months, not a full year. Confusingly, Falk et al. (2008) uses a 9-month growing season for eddy covariance work, the calendar

year for annual temperature calculations and a July-June water year for precipitation calculations. In this study, I explore the effect of employing the calendar year, the USGS water year and all other possible annual timeframes in the calculation of annual precipitation, annual productivity and annual rain use efficiency (RUE). Thomas et al. (2009) introduced the term “Hydroecological year” (HEY) for this and set the start date to November 21<sup>st</sup> for a forest plot in central Oregon.

Thomas et al. (2009) based their HEY start date solely on the average onset of widespread freezing air temperatures and justified this as preferable to using precipitation data because air temperature is a continuous dataset while precipitation is a sporadic dataset. They also stated that this accounted for frozen precipitation not being plant-available until it melted the following spring. This is highly analogous to the establishment of the USGS water year as starting on October 1<sup>st</sup> because any snowfall would be not be available for accounting purposes until it melted the following spring. This method of calculating the HEY is unsatisfactory because a “hydroecological year” should have its basis in both hydrology and ecology. Air temperature alone is a poor proxy for either of these two concepts except in specific circumstances and this necessitates increasing modifications to the methodology as it is applied to increasingly different ecosystems. A more generally applicable methodology is needed, particularly for regions that have only occasional freezing temperatures and have winter photosynthesis by evergreens, yet still have an observable seasonality to precipitation and productivity (Anthoni et al., 1999; Runyon et al., 1994).

As applied to their specific study area, Thomas et al. (2009) concluded that the concept of an HEY is vital to the understanding of water and carbon dynamics in a summer drought-stressed ecosystem and recognized that the application of the concept at other sites will require adjustments to their methodology to accommodate local conditions. An alternative to their methodology is to apply the principle of resource optimization to determine the day of year when annual productivity best fits annual precipitation.

One potential complication is that productivity logically lags behind precipitation as a function of soil hydrological and plant metabolic processes. Water-use-efficiency (WUE) studies (e.g. Gao et al. (2014); Reichstein et al. (2002); Tian et al. (2010); Zhu et al. (2013)) using some variation of eddy covariance derived measurements of productivity and evapotranspiration (ET),

$$WUE = \frac{Productivity}{ET} \quad [4.1]$$

mask the lag time because both measurements are linked through stomatal conductance. Therefore, any lag that applies to productivity also applies to ET to such an extent that one may be reliably modeled from the other. (Beer et al., 2009) Studies using a rain-use-efficiency (RUE) calculation (i.e. Bai et al. (2008) Huxman et al. (2004a)) such as

$$RUE = \frac{Productivity}{Precipitation} \quad [4.2]$$

are affected by this lag time between precipitation and productivity. With the exception of extreme conditions such that light precipitation does not result in additional plant available water, productivity is dependent on antecedent precipitation (Huxman et al.,

2004b) and therefore some lag time should be accounted for. A lag time calculated to maximize correlation between annual precipitation and annual GPP is presented along with the generalized method for determining HEY.

The objective of my research were to develop a procedure to compare the use of the USGS water year and the calendar year specifically, and all possible annual timeframes generally, for evaluating annual productivity as a function of annual precipitation in regions which receive little or no snowfall. The central criterion is to maximize the ability of the variation in annual precipitation to explain the variation in annual gross primary productivity.

## **Methods**

### *Site description*

The test data is from a karst site in central Texas, USA with the US-FR3 eddy covariance tower associated with Ameriflux (2013). The study area is a closed canopy wooded area on Freeman ranch, a 1700 ha research area near San Marcos, Texas managed by Texas State University—San Marcos. The area is a rocky outcrop of heavily jointed Cretaceous limestone. Soil is shallow in general, but may accumulate to a large degree in the joints and dissolution voids in the Karstic landscape (Jones, 2013; Veni, 2013). Mean annual rainfall is approximately 858 mm. Annual rainfall during the study period ranged from 319 mm in 2011 to 1740 mm in 2007, using the USGS water year definition. The mean annual temperature is approximately 20°C. There are few days when the temperature does not rise above freezing and consequently there is no accumulation of snow to melt in the spring. Two evergreens, Ashe juniper (*Juniperus*

*ashei*) and Plateau live oak (*Quercus fusiformis*), dominate the closed, interlocking canopy at approximately 8 meters height above the ground. The canopy is composed of approximately 49% juniper and 47% oak by number of individuals as calculated in Chapter II. A deciduous tree, Cedar elm (*Ulmus crassifolia*), is present in the canopy as well representing 4% of the canopy. Juniper dominates the understory species at 76%, followed by oak (4%), elm (2%) and the balance to non-canopy perennial species.

#### *Precipitation and flux measurements*

Precipitation data from an on-site tipping bucket raingauge (Texas Electronics, Inc., Dallas, TX, USA) were collected for calendar years 2004(4<sup>th</sup> quarter only)-2012. There were data gaps due to power failures that were filled manually from data collected at nearby research sites. Eddy covariance data were collected by a 3-D sonic anemometer (model CSAT3, Campbell Scientific Inc., Logan, UT) and an open-path gas analyzer (model Li-7500, LI-COR Inc., Lincoln, NE) both running at 10 Hz and mounted at 14 meters height above the ground. A prior analysis of the output of the EddyPro 3.0 program (LiCor, 2013) when processing data from this site in default configuration compared very favorably with four proprietary or in-house developed processing programs used previously. However, for the sake of uniformity, the results of these previous studies were not spliced together and all raw data was processed using EddyPro 3.0 running in default mode. EddyPro version 3.0 in default mode includes double axis wind rotation, block averaging, time lag optimization for maximum covariance, spike removal, absolute limits, WPL correction, high- and low- pass filtering, and sonic temperature correction for humidity as documented by LiCor (2013).

Flux data calculated during periods of low friction velocity ( $<0.15$  m/s), when the instrument was in the tower windshadow, during precipitation events or when there were indications of instrument errors were rejected during post-processing, resulting in data gaps. Other meteorological data collected included global irradiance (model LI-200 pyranometer, LiCor Corp, ), soil temperature (thermocouple between 2004 and 2007, model 5TM digital sensors by Decagon, Inc, Pullman WA, USA from 2008-2012) and relative humidity with air temperature (model HMP45C by Vaisala, Woburn, MA, USA) and were combined with the processed flux data and submitted to the online gap-filling and flux partitioning tool of Reichstein (2013) in order to obtain a continuous dataset for 8.25 years of carbon, water and energy fluxes. A combination of meteorological data, EddyPro processed fluxes, gap-filled data and partitioned data were submitted to and are available from Ameriflux as “Level 1” data. The gap-filling and flux partitioning tool has an optional algorithm for using the hyperbolic light response model which was not included in this dataset.

Gross primary productivity (GPP) was chosen for this study because it is the form of productivity most sensitive to water availability. The sensitivity of any form of net productivity (i.e. net primary productivity, net ecosystem productivity) is muted by the included respiration terms and respiration is greatly affected by temperature. The half-hourly data as uploaded to Ameriflux had some negative values for GPP and some positive night time values for GPP which were both considered spurious results and reset to zero. The final GPP dataset for this study differs from the Ameriflux level 1 dataset

by approximately 2 percent. The precipitation dataset is unchanged from the Ameriflux level 1 dataset.

*Annual data and determination of best fit start day of HEY*

To determine the best fit start day of the HEY, I used the equation,

$$HEY = \max_{1 \leq D \leq 365} (f(r_{(AP_D, AGPP_D, n)}^2, D)) \quad [4.3]$$

where the function  $f(\cdot)$  maps  $D$  to  $r^2$  ( $D \rightarrow r^2$ ); the function  $\max(f(\cdot))$  is bijective ( $D \leftrightarrow r_{max}^2$ );  $D$  is the day of the calendar year for which the function is being evaluated;  $r_{(AP_D, AGPP_D, n)}^2$  is the linear coefficient of determination between  $AP_D$  and  $AGPP_D$  for the day being evaluated given  $n$  number of years of daily data;  $AP_D$  is the annual precipitation in mm calculated for a particular day in a given year;

$$AP_D = \sum_{Day=-365}^{-1} Daily\ Precipitation \quad [4.4]$$

and,  $AGPP_D$  is the annual GPP in mm for the day being evaluated;

$$AGPP_D = \sum_{Day=-365}^{-1} Daily\ GPP. \quad [4.5]$$

Annual precipitation (mm) and annual GPP ( $g\ m^{-2}$ ) were calculated for each day of all years starting in the 4<sup>th</sup> quarter of 2005. Excel 2010 64-bit edition (Microsoft Corporation, Redmond, Washington) was used for this and all subsequent calculations. For the sake of standardization, annual precipitation was considered to be the sum of the rainfall occurring during the previous 365 days, without regard to the 2 extra days in the study due to leap years. Annual GPP was treated in an identical manner. A comparison

of the coefficient of determination ( $R^2$ ) from a linear regression analysis of annual GPP with annual precipitation for January 1<sup>st</sup> and for October 1<sup>st</sup> was made to find the start date which gave the best fit. This same analysis was performed for each day of year (DOY) to give a more complete picture of the annual variation.

#### *Lag adjustment*

A correlation coefficient (Pearson's  $r$ ) was calculated for annual precipitation and annual GPP starting together and then lagging GPP in a 1 day step-wise manner through 365 days. The lag time with the maximum correlation was found and all GPP data adjusted to form a lagged annual GPP dataset. Although the entire half-hourly dataset comprised 8.25 years, computation of annual precipitation and annual GPP removed a year of timeframe from consideration in the beginning and computation of a lag time removed a quarter of a year timeframe from consideration at the end of the process. As a result, there are 7 complete years in the paired dataset of annual precipitation and lagged annual GPP.

### **Results**

#### *Start date determination*

Considering only the two specific timeframes already discussed, the calendar year and the USGS water year, the effect of choosing between these when considering the effect of annual rainfall on annual GPP can be seen in Fig. 4.1. Note that in this case, using the USGS water year better captured the extremes of both annual precipitation and annual GPP and resulted in a better goodness of fit ( $R^2=.89$  vs  $.64$ ).

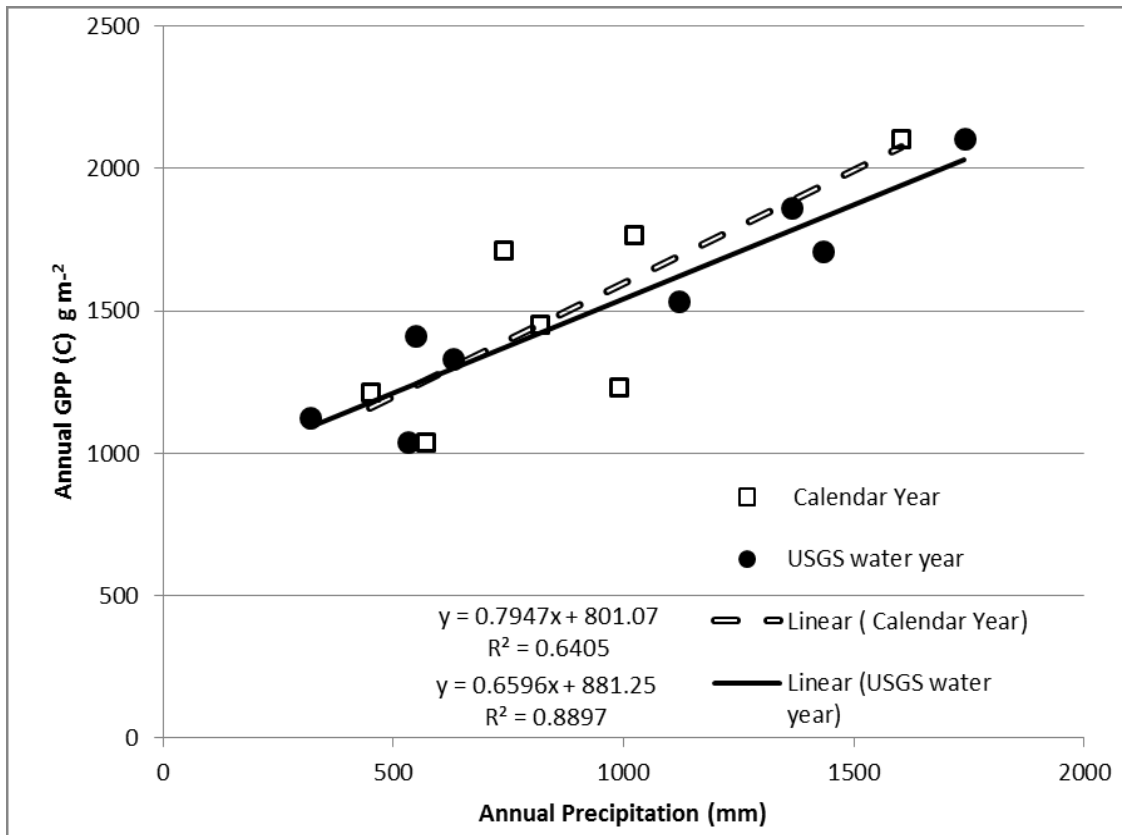


**Fig. 4.1 Comparison of AGPP and AP for the calendar year and the USGS water year.**

By performing this operation for each of the 365 possible start days of a year (ignoring “leap days”) and plotting goodness of fit ( $R^2$ ) against calendar days, it is possible to determine the calendar day on which starts the natural cycle of precipitation and growth (Fig. 4.4). The  $R^2$  values in Fig. 4.4 showed a high goodness of fit in the late 3<sup>rd</sup> quarter and early 4<sup>th</sup> quarter. The absolute highest value of 0.889 for the curve without lag occurred on day 274, or October 1st, which is also the start of the USGS water year.

### *Lagging*

Correlation (Pearson's  $r$ ) between annual precipitation and annual GPP with no lag adjustment was 0.73. Lagging GPP in a 1 day step-wise manner resulted in a smooth curve with a maximum  $r$  of 0.903 at a lag value of 91 days. (Fig. 4.4.) A marked improvement in goodness of fit can be seen in Fig. 4.3 as a result of lagging the GPP by 91 days. Figure 4.3 presents all possible annual timeframes resolved down to the day resulting in over 2500 value pairs on each graph.

The  $R^2$  statistic for annual precipitation vs annual lagged GPP showed a high goodness of fit in the late 3<sup>rd</sup> quarter to early 4<sup>th</sup> quarter of the calendar year in Fig. 4.4. The absolute highest  $R^2$  was 0.98 on day 263 which corresponded to September 20<sup>th</sup>. The  $R^2$  value for day 274 was 0.96.

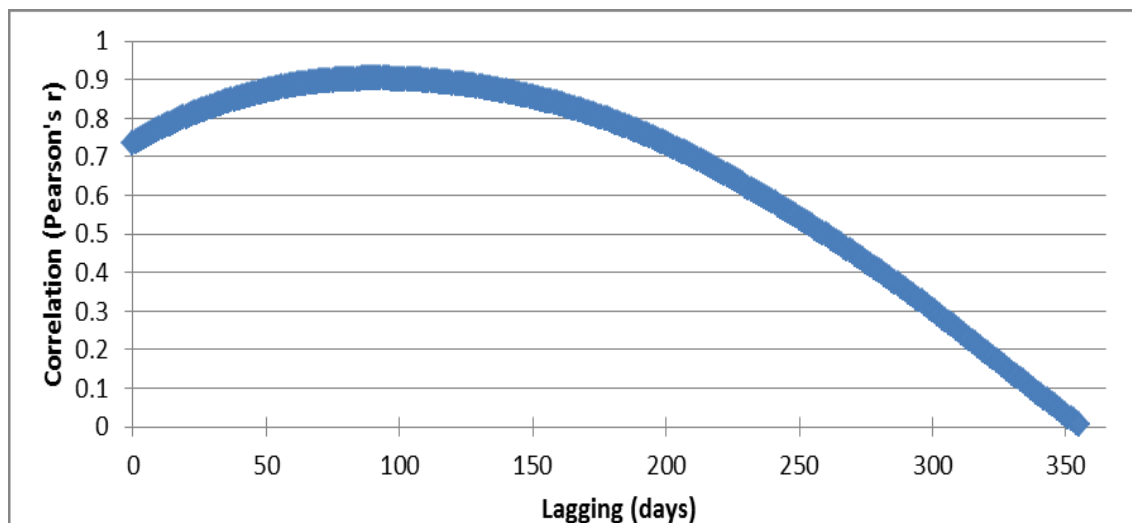


**Fig. 4.2 Correlation of annual precipitation and annual GPP with lagging. Maximum correlation was found with annual GPP lagging annual precipitation by 91 days.**

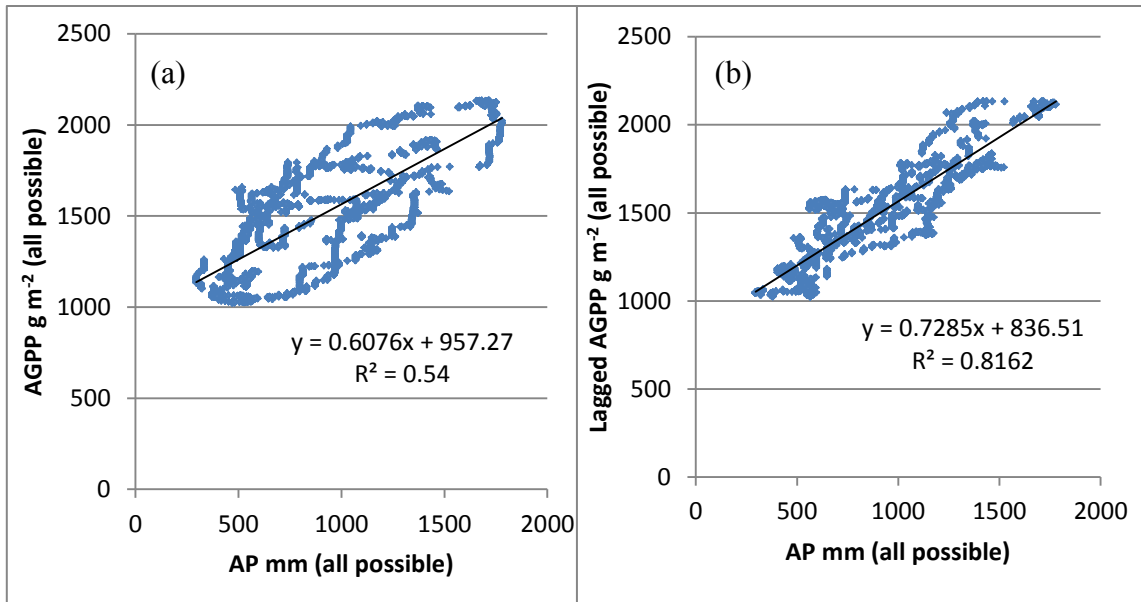


**Fig. 4.3** Comparison of unlagged annual GPP and annual precipitation (a), and lagged annual GPP and annual precipitation (b).

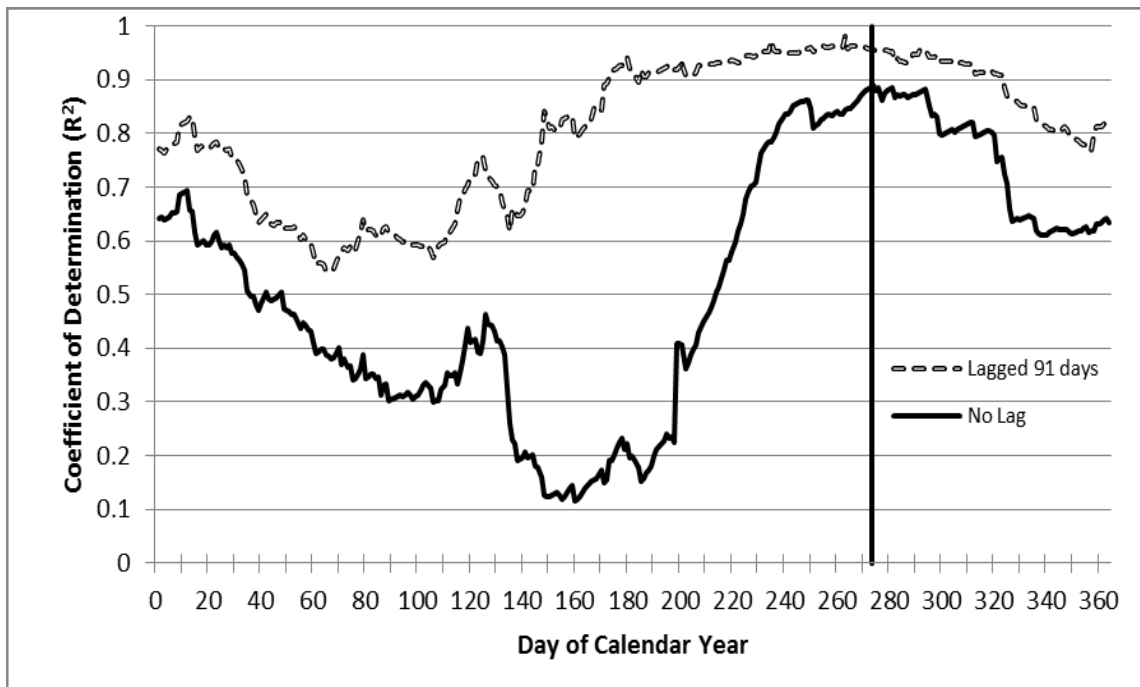


**Fig. 4.4** Coefficient of determination throughout the calendar year between AP and AGPP. Dark vertical line at day 274 designates the beginning of the USGS water

However, the curve was fairly flat at that point with a  $R^2$  over 0.95 from August 19th to October 8th, encompassing the start date of USGS water year for the non-lagged variable of annual precipitation. August 19th to October 8th corresponds to November 18th to January 7th for the 91-day lagged variable of lagged GPP, encompassing the start date of the calendar year for that variable. Note that lagging improved goodness of fit regardless of the chosen start date.

#### *Rain use efficiency*

RUE decreased in a non-linear fashion with increasing AP (Fig. 4.5). Using the calendar year and no lagging, variation in AP explained 66% of variation in RUE using a power series trendline. However, it improved to 98% using the USGS water year and lagging GPP by 91 days.

#### **Discussion**

Data from both precipitation and productivity were used to determine the HEY start date. That the date in this case fell on exactly the USGS water year start date and has such a high goodness of fit indicates that the ecosystem productivity at the test site was tightly constrained by precipitation. Without applying a lag adjustment, the variation in precipitation explained 89% of the variation in GPP. However synoptic data from natural systems can misalign cause and effect in ecosystems when the effect is delayed. Productivity in this ecosystem lagged precipitation by 91 days when using an annual timeframe for evaluation, and a goodness-of-fit of 0.96 was obtained by lag adjusting annual GPP. This leaves virtually no room for other causes of variability in annual GPP. There do not seem to be any substitutes for precipitation such as run-on or

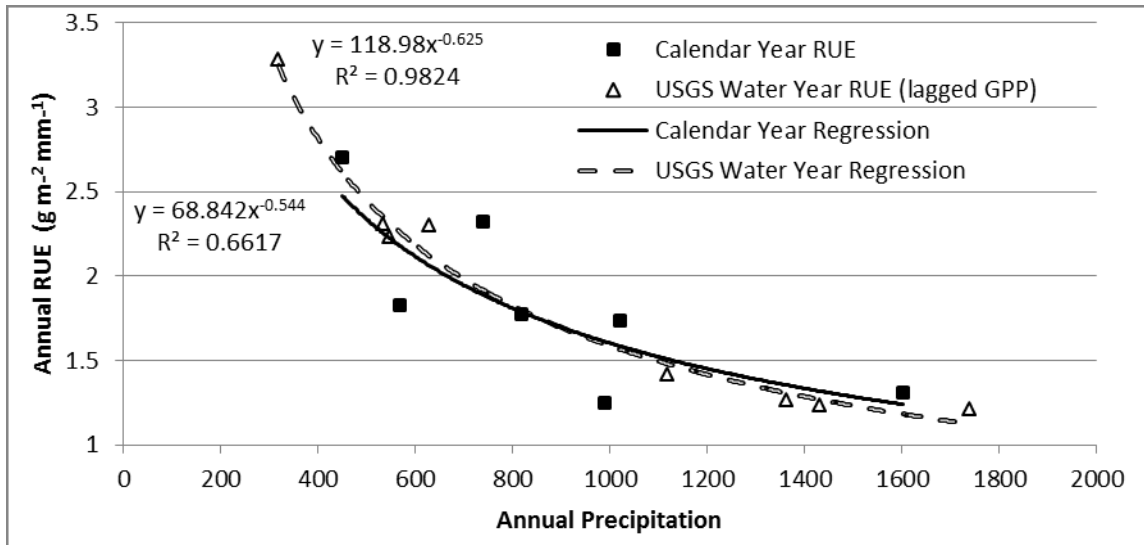


**Fig. 4.5 Annual rain use efficiency as a function of annual precipitation.**

a phreatophytic strategy. Other potential causes of variation such as light availability and episodic diseases or insect infestation did not appear to manifest themselves during the period of available data or they were contained within the remaining 4% unexplained variation. A close inspection of the extremes of Fig. 4.1 reveals that there was no threshold at low values, nor any saturation plateau at high values. Speculatively, this is indicative that the species which make up the forest are well adapted for this climate and are not living on the edge of their range.

Annual RUE shows a similar problem of a low goodness of fit of 0.66 as a function of AP when using a calendar year timeframe without lag adjusting data (Fig. 4.5). A high goodness of fit is expected in this situation because of self-correlation between Annual RUE and AP where AP is also a divisor in Annual RUE. A negative exponential trend line is also expected in this type of display. Despite the problem of

self-correlation, this is a typical manner to display this data (e.g. Fig. 5 in Bai et al. (2008), Fig. 5 in Lauenroth et al. (2000), Fig. 1 in Fensholt et al. (2013), Figure 1a-inset in Huxman et al. (2004a), and Fig. 5 in Prince et al. (1998)). In particular, Bai et al. (2008) reported RUE as a function of AP for two ecosystems on the Mongolian Steppe with  $R^2$  values of 0.24 and 0.29 using a linear fit trendline. Low goodness of fit values typically mean that there is an unknown source of variation. However, in the present study, using the USGS water year timeframe and lag adjusting GPP showed that most of the previously unexplained variation is an artifact of timing. A very tight negative exponential relationship is shown in Fig. 4.5 after the timing adjustments.

Antecedent conditions govern whether plants are physiologically ready to use rain when it falls (Schwinning et al., 2004). When the precipitation begins to fall after a summer drought, plants lack sufficient structures to take maximum advantage of it. Some lagging can be attributed to shriveled up root hairs and old, inefficient leaves (Huxman et al., 2004b). However, soils will store the water and make it available later in the season once the plants have grown new roots and put on new, more efficient leaves. In temperate climates with long periods of freezing weather, the lagging is due to the storage of water in snow rather than in a plant available form. In sub-tropical deciduous forest stands, the trees are not equipped to utilize precipitation for productivity after leaf-fall and before bud-out in the spring, regardless of the temperature. These diverse causes of productivity lagging precipitation contributed to the gradual approach to and decline from the maximum correlation value seen in Fig. 4.3. If there had been a single, consistent cause, then Fig. 4.3 should have shown a sharp

peak. Consequently, the calculation of a 91 day lag time presented here is a composite annual value which may have unwanted consequences when analyzing smaller timescales such as daily, weekly and monthly RUE. Lag time is greater than 91 days as storage of water is increasing and the ecosystem is ramping up its response. Lag time is shorter than 91 days as storage of water is depleted and the ecosystem is being constrained. Applying the 91 day annual lag adjustment to a short period of time when storage is low and lag times are short will result in the ecosystem apparently responding to an increase in precipitation before it happens. Therefore, lag adjustments should be applied with some caution, perhaps with a variable temporal window.

In an idealized situation of annual precipitation being a sine wave and annual GPP being a lagging out of phase sine wave, lag adjusting annual GPP will result in a constant value of 1 for  $R^2$ , regardless of the start date. This is clearly not the case in Fig. 4.2 as the  $R^2$  value for the lagged annual GPP ranged from a low of approximately 0.54 to a high of 0.98. The choice of the start DOY can have a greater effect on annual goodness of fit calculations than lag adjustments. However, both the lag time calculation and the HEY calculation were used in this study to maximize the ability of the variation in annual precipitation to explain the variation in annual GPP.

This is presented as a general method for calculating a site-specific start DOY for a HEY, and analysis of annual RUE. If this method were applied to other ecosystems, the results would be different. For instance, a grassland should have a much shorter lag time as annuals typically respond to precipitation much more quickly than perennials (Huxman et al., 2004a; Huxman et al., 2004b). In an ecosystem dominated by

phreatophytes, the lag time may not be discernable and the goodness of fit may be poor (Huxman et al., 2004a).

### **Conclusion**

Using this method to calculate the calendar day of the year on which to start the HEY for a particular ecosystem provides a justification for the choice of the start day for an annual timeframe, and better captures the extremes of data while simultaneously tightening the goodness of fit in describing the response in annual GPP to annual precipitation. Lag adjusting GPP for maximum correlation to annual precipitation further strengthens the explanatory power of annual precipitation to annual GPP. The method requires a considerable amount of very specific data to analyze and access to computers which can handle the computational requirements. However, flux tower data is increasing and adequate computers are becoming more commonplace, allowing this method to be used on a wide variety of ecosystems.

CHAPTER V  
CARBON FLUX PARTITIONING BETWEEN TWO SPECIES IN A RAPIDLY  
CHANGING FOREST

**Introduction**

Forests represent a growing carbon pool which can be measured using eddy covariance methods and also by biometric methods. Although the eddy covariance method is relatively new compared with biometric methods, the credibility of the eddy covariance estimates is increased when it converges with those of biometric methods. The strength of the eddy covariance method is in the estimation of whole-ecosystem fluxes from a vantage point above the ecosystem (Baldochi, 2003). This overall estimate must be separated into component processes such as above ground biomass carbon allocation, below ground biomass carbon allocation, storage carbohydrates, reproduction, leaf replacement, autotrophic respiration and heterotrophic respiration in order to be directly comparable to a biometric estimate. In a system with codominant trees, the species specific contributions need to be known to understand carbon dynamics (Bendevis et al., 2009). Conversely, the strength of biometric measurements is in the estimation of component fluxes from a vantage point within the ecosystem. These estimates must then be summed to be directly comparable to eddy covariance derived estimates. The disparate approaches each have independent sources of error (Curtis et al., 2002; Luysaert et al., 2009) and a comparison between them can lend insight into

both the methods and the processes (fluxes, sequestration, productivity, respiration, etc.) regardless of the degree of convergence.

Net ecosystem exchange (NEE) of carbon dioxide derived from eddy covariance methodology is the whole ecosystem measure of carbon gain or loss without regard for individual ecosystem component contributions. It represents the combination of gross primary productivity (GPP) and ecosystem respiration (Re) or, more simply, carbon gain and carbon loss. Although GPP is fundamentally generated in the photosynthetic apparatus of plants, it is identified with the plant component that the photosynthate is allocated to. It may be allocated to leaf, stem, fruit, trunk and roots. In the context of the ecosystem, the fate of the photosynthate may also be herbivores, carnivores and decomposers using the carbon gain concept. Each of these components also contributes to Re as a result of metabolizing the photosynthate back to CO<sub>2</sub> and H<sub>2</sub>O. Many component contributions to NEE are assumed to be negligible or zero in a stable climax ecosystem. For example, soil carbon gain is assumed to equal soil respiration and overland carbon influx in the digestive tracts of migratory animals is assumed to be equal to carbon efflux of those same or equivalent animals. The disappearance of carbon dioxide in the process of chemical weathering of limestone to create karst topography is offset to some extent by the reverse process during evaporation. However, each of these component contributions may be non-negligible in certain circumstances. Soil carbon gain may exceed soil respiration in a sub-climax ecosystem undergoing a woody encroachment stage as new roots, root exudates and leaf litter build up faster than

decomposition. Agricultural practices remove carbon unidirectionally from the ecosystem to the supermarket shelves.

Chemical weathering of limestone bedrock is conceptually very problematic when using eddy covariance techniques for two reasons. First, the eddy covariance method does not work during precipitation events. Data collected during those times are discarded and replaced with values modeled on light and temperature. However, the water carries CO<sub>2</sub> from the atmosphere into the limestone where it reacts. It can also displace air enriched with CO<sub>2</sub> derived from soil respiration out of soil pores and dissolution voids into the atmosphere. The ratio of dissolution-gain to displacement-loss of CO<sub>2</sub> in a karst landscape is unknown, but the implicit assumption of the eddy covariance method is that they cancel out. If there is sufficient precipitation to cause runoff or recharge, then dissolved carbonates, including the CO<sub>2</sub> used to dissolve them, will be exported from the system. The source of the CO<sub>2</sub> then becomes important. Atmospherically sourced CO<sub>2</sub> in the runoff is just passing through without being quantified in any eddy covariance derived flux calculations due to the lack of measurements during rain events and the lack of measurements in the aquifer or surface flows. However, CO<sub>2</sub> sourced from biological sources (e.g. respiration) was initially accounted for as negative NEE (and therefore positive NEP) during photosynthesis before the rain event, but completely missed during the during the respiration stage because the CO<sub>2</sub> was exported from the system in a form that is not measured by eddy covariance. Table 5.1 summarizes the problems listed above.

Many researchers have inquired as to whether estimates made using the eddy covariance method have any correlation with biometrically derived measurements. The general consensus is that there is a convergence between biometric estimates and eddy covariance estimates using multiple years of cumulative data. Studies with 5 years (Gough et al., 2008), 7 years (Curtis et al., 2002) and 10 years (Baldocchi et al., 2005) of cumulative data have been reported. A common, easy and economically important biometric measurement is diameter at breast height (dbh). When coupled with allometric equations such as developed by Jenkins et al. (2003), above- and below-ground biomass can be estimated. Wood, above-ground live biomass (bm) without the leaves, represents the unidirectional flux of carbon dioxide incorporated into biomass through photosynthesis and is the most cumulatively conserved component of the carbon cycle. As such it is the ideal component for comparing multi-year estimates using eddy covariance and biometry. Since the molecular weight equivalent of wood biomass is different from the molecular weight of carbon dioxide, they will be expressed in terms of their carbon content (bm-C and CO<sub>2</sub>-C) in this chapter.

Net ecosystem exchange (NEE) is a measurement of the bidirectional flux of CO<sub>2</sub>-C moving into and out of the atmosphere with a sign convention that the atmosphere is gaining CO<sub>2</sub>-C when NEE is positive and losing it when NEE is negative. This sign convention signifies that NEE is net atmospheric exchange in concept. Net ecosystem productivity (NEP) is the term used to show the amount of CO<sub>2</sub>-C that has been stored in the ecosystem. In general practice, NEE is used to describe short term fluxes (minutes to days) while NEP is used to describe long term flux (weeks to years).

In this study the timeframe for NEP is annual, specifically the USGS water year. The sign convention is that NEP is positive when the ecosystem is gaining carbon (such as when photosynthesis exceeds respiration) and negative when the ecosystem is losing it (when respiration exceeds photosynthesis). NEE and NEP are equivalent in magnitude over the time period (Curtis et al., 2002) while opposite in sign.

**Table 5.1 Situational sources of error when using eddy covariance.**

Cause of error	Mechanism	Effect
Agriculture	Unidirectional export of biomass. Reduces actual soil respiration.	Overestimates NEP
Woody encroachment	Imbalance between soil carbon gain and soil respiration.	Underestimates soil carbon gain.
Precipitation	Shuts down eddy covariance	May either over- or under-estimate NEP depending on the gap-filling model and light and temperature.
Displacement	Flux of CO <sub>2</sub> rich air not measured due to shutdown of eddy covariance during precipitation.	Overestimates NEP
Chemical weathering	Time-displacement of unmeasured storage and measured release of CO <sub>2</sub>	Underestimates NEP. Overestimates soil respiration.
Runoff and recharge	Unidirectional export of mineralized CO <sub>2</sub> with ambiguous origin.	Neutral if CO <sub>2</sub> origin is atmospherically derived, overestimates NEP if CO <sub>2</sub> is derived from respiration.

The limitations, shortcomings and corrections intrinsic to the eddy covariance method itself have been extensively covered over the past 20 years (Baldocchi, 2003; Burba, 2013; Ham and Heilman, 2003; Massman, 2000; Schotanus et al., 1983; Twine et al., 2000; Webb et al., 1980) and are not directly addressed herein. Rather, the present research question is whether a modern eddy covariance system with a full suite of corrections for intrinsic problems applied can adequately predict the wood increment component of NEP for this ecosystem, and be divided between contributions made by two codominant trees with very different life histories and drought survival strategies.

## **Methods**

For this study, NEP derived from eddy covariance measurements was compared to biomass increment derived from biometric measurements and allometric equations.

### *Eddy covariance estimate of NEP*

The eddy covariance measurements, corrections, filters and gap-filling were the same as in Chapters III and IV. For this investigation, the gap-filled NEE column was summed on an annual basis using the USGS water-year time frame in a manner consistent with that was used for gap-filled LE and GPP columns in Chapters III and IV, respectively. Annual NEE was transformed into NEP by reversing signs.

### *Dendrochronological estimates of wood increment*

Wood increment was estimated in two ways; by using the values calculated in Chapter II for above-ground biomass, and by subtracting leaf weight from individual trees and recalculating the above-ground biomass equations in Chapter II. Removing the leaf weights introduced more variability into the regression equations and the resulting

least-squares best fit regression estimated slightly greater above-ground biomass than without the leaves. Since subtracting the leaves gave confusing and only slightly different results, the entire above-ground biomass increment from Chapter II was used in this study as wood increment. To make it more directly comparable to the biometric estimates which only considered above-ground biomass, biometric increment was increased according to a 20% rule-of-thumb (Curtis et al., 2002) for below-ground biomass. The results were divided in half to express biomass on the basis of carbon content (Black et al., 2007; Blackard et al., 2008; Gough et al., 2008)

#### *Light study*

A light study was attempted on the 20 study trees to document light penetration under the study trees crowns before and after harvest. Two identical quantum light sensors were connected to a Campbell Scientific CR21x datalogger, calibrated daily in a side-by-side comparison using ambient light and then one was lifted above the canopy on a long pole while the other was steadily walked from one side of the sample tree's crown to the other side twice, from north to south and from east to west. Data were collected at 10Hz, beginning and ending times were noted manually and the study data were extracted from the datalogger record during post-processing using the field notes as a time reference. Several technical and procedural failures discovered during post-processing resulted in the abandonment of the before and after harvest comparison. However, four of the attempts to collect light penetration before harvest were successful.

## Results

The seven year cumulative carbon sequestration estimates for juniper, oak and the combination of the two are shown in Fig. 5.1 together with the eddy covariance derived estimate of NEP. The standard error of the mean population density estimate shown in table 2.3 was used to construct the error bars shown in Fig. 5.1. About half of the NEP was unaccounted for by the biometric data as shown in Fig 5.2. Figure 5.3 details the whole ecosystem response to annual rainfall using the USGS water year as a reference. The four successful light penetration readings taken before harvest had an average value of 10% light penetration (range: 5% - 30%).

## Discussion

The timespan of 7 years does not facilitate comparisons with other literature and so the equivalent annualized values are given as 1.11, 0.29, 1.40 and 3.08  $\text{Mg ha}^{-1}\text{yr}^{-1}$  for oak, juniper, total and NEP, respectively. The value of NEP is similar to the values of 3.2 and 2.7  $\text{Mg ha}^{-1}\text{yr}^{-1}$  found by Anthoni et al. (1999) for a semiarid evergreen forest in Oregon as well as with 2.4 to 3.8  $\text{Mg ha}^{-1}\text{yr}^{-1}$  found by Ehman et al. (2002) for a “mid-latitude mixed hardwood forest” in Indiana. Conversely, the values for the biomass increment of oak, juniper and their total compares more closely to the range of 0.8-1.98  $\text{Mg ha}^{-1}\text{yr}^{-1}$  found by Gough et al. (2008) for a deciduous forest in Michigan.

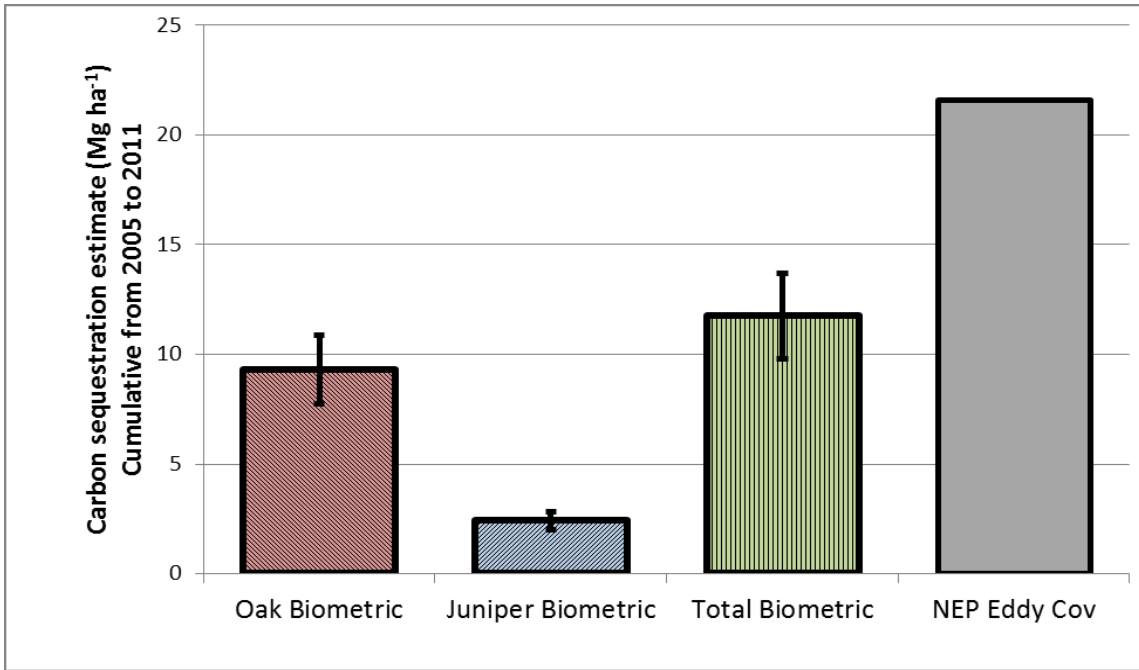


Fig. 5.1 Carbon sequestration estimates.

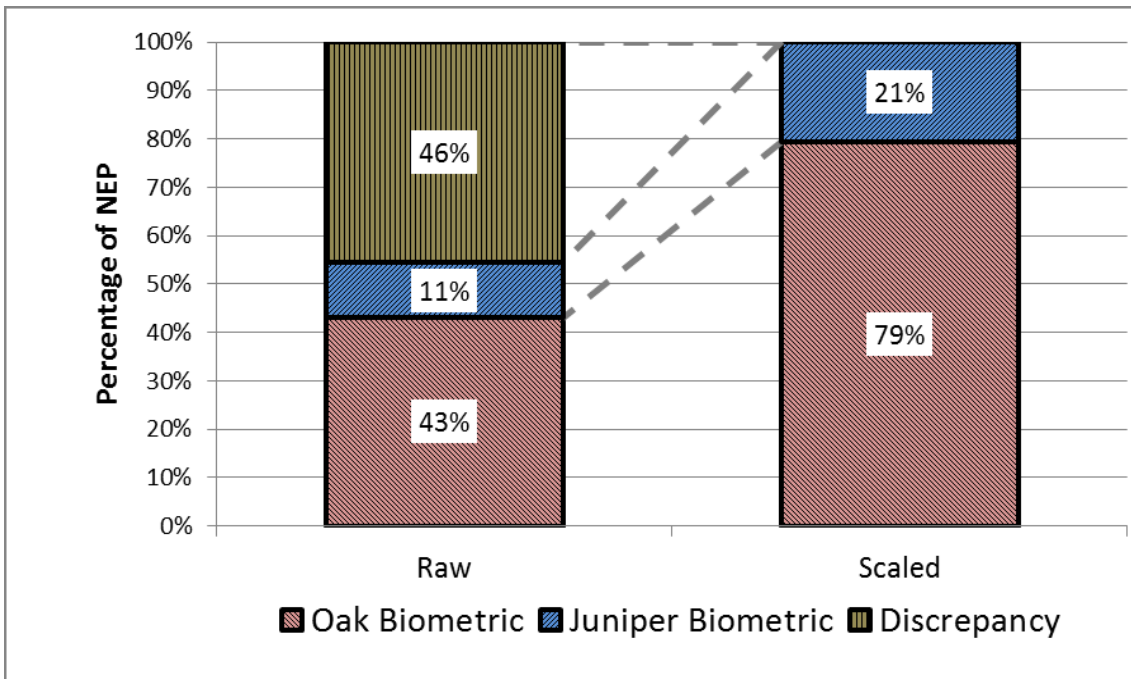
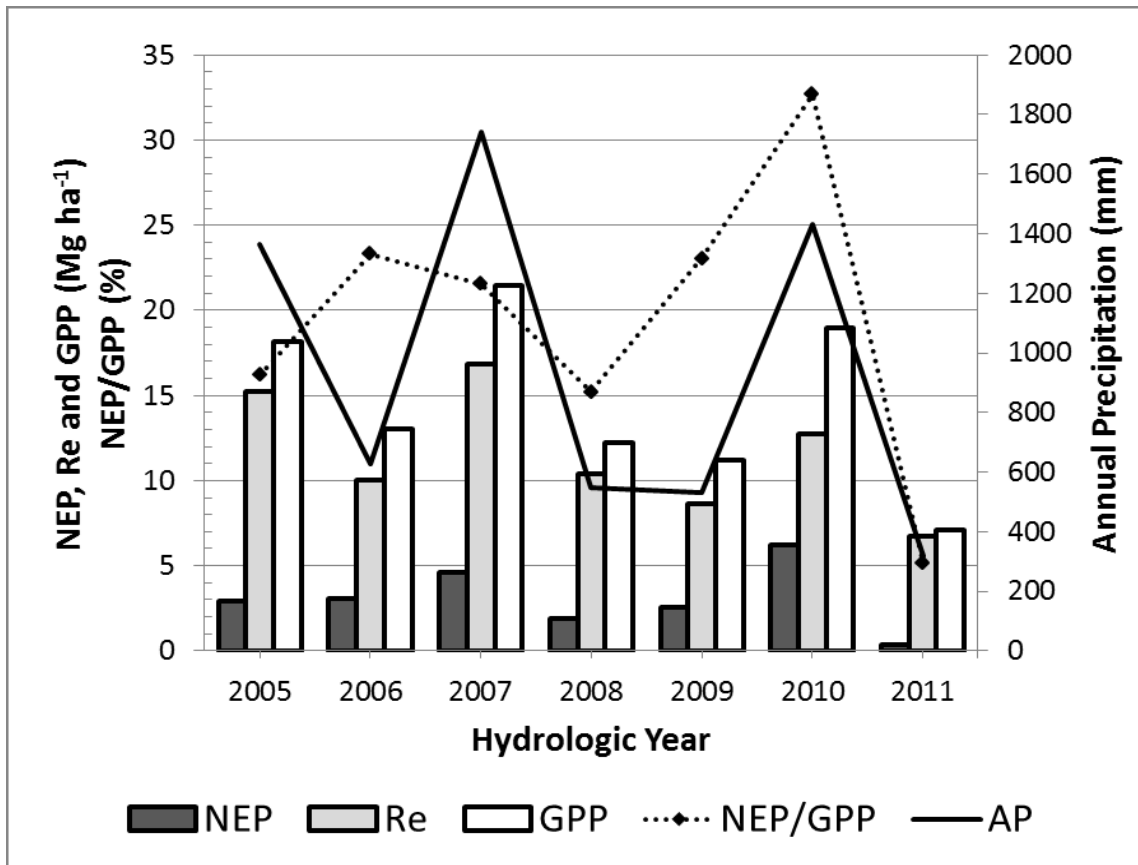


Fig. 5.2 Partitioning and scaling of NEP components.



**Fig. 5.3 Carbon balance of eddy covariance measurements.**

As seen in Fig. 5.3, the eddy covariance derived estimates of NEP, GPP and Re all generally followed annual precipitation ( $r=0.81$ ,  $0.98$  and  $0.95$ , respectively) using the hydrologic year timeframe. This highlights that the ecosystem is water-limited and that the dominant trees do not have access to laterally transported water. Water-limitation is likely responsible for the low NEP of  $3.08 \text{ Mg ha}^{-1}$ . NEP averaged 20% of GPP but annual precipitation was poorly correlated to this percentage ( $r=0.5$ ).

It is striking in Fig 5.3 is that Re averages 80% of GPP while NEP averages 20%. The Re percentage is a little higher than the 76% found in a 12 year study on 80 year old plantation oaks by Wilkinson et al. (2012). GPP values are also higher than the ~3 to 17 Mg ha<sup>-1</sup> annual values given for oak and juniper (although different species and locations) in a metastudy performed by DeLucia et al. (2007). Randerson et al. (2002) make the point that NEP should include non-biotic CO<sub>2</sub> flux (which this does via the eddy covariance methodology) and non-CO<sub>2</sub> carbon flux such as inorganic and organic carbon in runoff and percolation (which this study does not include). In general, autotrophic respiration accounts for about 47% of GPP (Randerson et al., 2002), so when ecosystem respiration is 80% of GPP, then 33% of GPP is being balanced by heterotrophic respiration. It is also possible that both Re and GPP were inflated by non-biotic CO<sub>2</sub> flux because the GPP calculation was dependent on Re values which in turn were dependent on NEP values. A non-biotic source of CO<sub>2</sub> flux (chemical weathering of limestone) would have been assigned to Re in the data processing and GPP would then have been increased to achieve mass balance of carbon. This hypothesized non-biotic component may help explain the apparently high Re and GPP of this ecosystem which incongruously had the relatively low average annual NEP of 3.08 Mg ha<sup>-1</sup>.

The biometrically estimated biomass increment only accounted for 65% of the eddy covariance estimate of NEP over a 7 year period. This failure to converge is a departure from the experience reported by other authors and requires further inquiry. Either the NEP derived from eddy covariance was overestimated or the biometric and allometric components were underestimated, or both.

### *NEP*

In Chapter III, annual evapotranspiration (ET) tracked annual precipitation very closely in the drier time periods. Confidence was gained regarding the operation and processing of the eddy covariance values due to the convergence of those two values. Precipitation, as measured by a rain gauge independent of eddy covariance, was the input to the equation and ET was the output. The situation is reversed in this study with the supply variable ( $\text{CO}_2\text{-C}$ ) measured by the eddy covariance equipment and the product (bm-C) measured independently. If NEP has been overestimated, it might be due to faulty data collection, faulty application of the method or faulty data processing. However, the high goodness of fit between annual precipitation and annual ET argues against those potential causes since the annual ET calculation was dependent upon the same data collection, handling and processing as NEP.

The situational sources of error summarized in table 5.1 include 4 sources of error which could potentially have caused an overestimation of NEP. Of these, agriculture can be dismissed as a cause in this ecosystem because the forested area in the eddy covariance footprint is too dense and has too little food appropriate for cattle or wildlife. No other agricultural practices have been occurring there. The effects of the remaining three items (precipitation, displacement and runoff/recharge) are unknown.

### *Biometric measurements*

The biometric study was very basic although labor intensive. Only canopy trees were measured because they intercepted the most light, but understory trees far outnumbered canopy trees. The 10% light penetration, although not definitive due to the

low sample size, is higher than the range given by Montgomery and Chazdon (2002) of 0.2% - 6.5% and indicates that the understory is receiving more light than might be expected when discussing a closed canopy forest. Also, the light penetration values in the study of Montgomery and Chazdon (2002) and in this study are for the forest floor and for 1.4 meters, respectively. Much of the understory was taller than 1.4 meters and potentially exposed to even more light. Therefore, photosynthesis by the understory may account for a significant portion of the discrepancy between the eddy covariance estimate of NEP and the biometric estimate of bm increment. Other possible causes of a low biometric bm increment estimate are:

--The 20% “rule of thumb” for below ground biomass may be inaccurate for this study if these species allocate more carbon to root development than is typical. Thomas et al. (2009) assumed 25% in their study on Ponderosa pine.

--The “woody encroachment” situational source of error in Table 5.1 not only applies to belowground carbon allocation, but also to leaf litter buildup. Davidson et al. (2002) suggest that leaf litter is roughly equal to one half of the value for below ground carbon allocation. However, this only applies in situations where new leaf-fall is not balanced by old leaf-fall decomposition. There were no direct measurements of leaf-fall or decomposition in this study. A rough relationship to below-ground carbon allocation, which itself is a rough relationship to above-ground biomass, is too tenuous to explicitly quantify.

--Tree density may have been underestimated due to bias in the choice of transect location. Accessibility by truck was a major factor in transect location choice so that tree samples could be transported to scales to be weighed.

--Elm accounted for 4% of the canopy community, but was ignored in the biomass calculations.

--The tree density estimates' upper error bars may be a better estimation of the mean density than the mean.

## **Conclusions**

The values found for both biomass increment and for NEP were consistent with values found for other forests even though there was a 46% discrepancy. A “general consistency” was declared by Ehman et al. (2002) when comparing biometric and eddy covariance estimates of NEE with a discrepancy as high as 31%. This study had a higher discrepancy, but several factors were identified which indicated that the error was in the biomass increment value and not in the NEP value. This may be useful in future studies for greater and more accurate parameterization of the estimates. Until those future studies can be realized, a scaling factor of 1.85 applied to tree density is required to force convergence of the two estimates, assuming that the eddy covariance estimates of NEP were accurate. Scaling in this manner impacts the understanding of the maturity of the forest and arbitrarily doing so is fraught with the possibility of underestimating useful timespan remaining for this forest to be a carbon-sink. This is because a fully matured forest will achieve equilibrium between photosynthesis and respiration creating an expectation that NEP will be close to zero in an old, mature forest (Davidson et al.,

2002; Raich and Nadelhoffer, 1989). It was shown by Law et al. (2003) in a chronosequence of Ponderosa pine that NEP is negative during the seedling stage of afforestation (due to decomposition of wood residues from the previous crop not being balanced by photosynthesis of the new seedlings), rises in a young forest, rises still more in a mature forest and then plummets in an old growth forest. If the NEP value found in this study is more accurate than the biomass increment as postulated, then the forest is closer to exhausting its capacity to act as a carbon sink.

Partitioning of NEP between two co-dominant species in this study was made on a cumulative multi-year basis and resulted in 21% for the juniper and 79% for the oak when the biometric estimates are scaled up to the eddy covariance estimate.

Corroboration of this was sought within the eddy covariance data by analyzing half-hourly, daily and monthly data for a bimodal pattern in carbon flux and ET. A pattern was found on clear days whereby NEP in the early morning increased to the daily maximum and then decreased by late morning to about 2/3 of the maximum value. For the rest of the day it slowly declined to about half of the maximum value when light failed and NEP went to zero. Speculatively, the early daylight peak represents photosynthesis by oak trees which can rapidly open and close stomata while the slow decline after the initial peak represents photosynthesis by juniper which have slow opening and closing stomata. Unfortunately, this pattern was inconsistent (occurring perhaps 1 out of 5 clear days), the magnitude of the peak was smaller than might be expected for such a dominant tree and the pattern was non-existent on cloudy or partly cloudy days. This early morning peak was interesting, but ultimately the component

parts could not be distinguished. Consequently, biometric measurements were indispensable for partitioning NEP into species specific components. This coarsened the timescale for the analysis to at least a year and ultimately to the full seven years of available data due to the difficulty in reading the oaks' annual rings.

## CHAPTER VI

### CONCLUSIONS

This study demonstrates that understanding the history of a forest stand is vital to understanding its carbon and water dynamics. Historical fire suppression, hunting and agricultural practices have at times favored oaks and at times favored junipers. The development of the forest itself out of a savanna has fostered both species in a runaway trend due to increased fire resistance and decreased herbivory, both of these being due to the shading out of grass species. Water limits the ecosystem as a whole and since karst geology generally prevents perennial surface streams, changes in water storage and water use efficiency are closely coupled with water use by trees. The early chapters of this dissertation examined fundamental attributes of the forested study area such as the species-age structure of canopy-forming trees and an appropriate annual timeframe for data analysis. These attributes were used in the final chapter to partition carbon and water flux between the two species. This work draws from, expands on and adds to previous studies performed at this site, at nearby sites and at similar sites.

#### **Relationship to Previous Studies**

This study expands upon the leaf-level study of Bendevis et al. (2009) on the same stand of trees. They found that juniper had lower carbon assimilation, transpiration rates and stomatal conductance than oak. When coupled with the result found in Chapter II of this study that juniper only accounts for 14% of the standing biomass and the result found in Chapter V of this study that juniper only account for 21% of the annual biomass

increment, it appears that juniper and oak are only codominant in terms of density. Oak appears to be clearly dominant in terms of standing biomass, carbon flux and, since carbon assimilation is tightly linked to ET through stomatal conductance, it follows that oak is also the dominant water user.

Bendevis et al. (2009) found that juniper photosynthesis was more influenced by antecedent rainfall than oak. They also found that oak photosynthesis exceeded juniper photosynthesis under all patterns of rainfall even though juniper water-use efficiency exceeded that of oak. I found in Chapter II of this study that this is also the case for tree ring formation. In the tree-ring record, the oak tree ring widths did not correlate to rainfall patterns, but juniper tree ring widths did. This is exceedingly puzzling because it is well established in Chapters III and IV of this work as well as in numerous other publications that this ecosystem is water limited. It is to be expected that the species contributing the overwhelmingly majority of the annual biomass increment would likewise be water limited but it shows no signs of this limitation at the leaf level or in its collective annual biomass increment.

Bendevis et al. (2009) distinguished between the response of the oak trees in a closed woodland and those in an open savanna. They found that the open savanna oak trees responded to antecedent rainfall patterns while the closed woodland oak trees did not. I also found this in comparing the preliminary dendroclimatological study mentioned in Chapter II with the main dendroclimatological study. The rainfall signal that was evident in the savanna oak tree rings was almost completely lacking in the closed forest oak specimens. This indicates that water availability is not a limiting factor

in the forest while the presence of a precipitation signal in the savanna oaks indicates that this species does respond to precipitation. This is concordant with the findings of Elkington et al. (2014) that, in general, the trees of any species were least affected by precipitation on the deepest savanna soils and most affected on shallower soils with the exception that the oaks had equal access to water between the savanna site with the deepest soil and the forest site. Combining all these lines of evidence, it appears that the oaks of this forested area do have perennial access to water, but that its use is restricted. In this case, “perennial” does not have the same meaning as “stable” in that stability implies lack of change whereas perennial availability does not preclude that the water may become increasingly difficult to obtain or to use.

### **Broader Implications**

A regionally important finding in this dissertation is that a precipitation threshold of approximately 520 mm is needed after October 1<sup>st</sup> before there is water available for run-off or recharge, subject to not exceeding percolation limits of the soil. Also, the new method using eddy covariance data to estimate the water holding capacity of the soil and rock in this environment can be used for better modeling of water availability of this area.

The empirical calculation of the local water year (which in this case coincided with the USGS water year) and the local HEY together with lag optimization are methods which researchers worldwide can use with existing and future ecosystem data to remove variation in water and carbon budgets caused as an artifact of timing. This increases the sensitivity of the analysis to other sources of variation. The effect of

smaller variations such as that caused by disease outbreaks, insect infestation, exotic invasions and climate change can be investigated without being overwhelmed by the effect caused by the change in storage of the plant available water.

### **Future Directions**

The most puzzling finding of this dissertation is that the oak trees dominated CO<sub>2</sub> flux and water flux over the cumulative 7 year period without their tree rings responding to precipitation even though both of these fluxes clearly changed in response to precipitation as measured by eddy covariance. This needs to be resolved to more clearly understand annual and sub-annual carbon allocation and water use in the oaks. Since juniper tree rings clearly respond to precipitation and junipers dominate the understory, could the understory (together with the canopy juniper) be responsible for the variation seen in the eddy covariance data?

The site is no longer an active eddy covariance site and its tower was dismantled in the summer of 2014 at which time a tremendous infestation of juniper bud worm was observed. The infestation had caused the normally green or blue-green junipers to appear primarily brown with a tinge of green. The impact of this type of phenomenon on water use and productivity can be investigated within this dataset now that the goodness of fit between precipitation and ET and GPP has been optimized. Previously, the effect would have been undetectable within the previously unknown effect of the change in water storage. Although the site is no longer active, research may be conducted on phenomena which occurred within the study time period.

## REFERENCES

- Abrams, M.D., Ruffner, C.M., Morgan, T.A., 1998. Tree-ring responses to drought across species and contrasting sites in the ridge and valley of central Pennsylvania. *Forest Science*, 44(4): 550-558.
- Afinowicz, J.D., Munster, C.L., Wilcox, B.P., 2005. Modeling effects of brush management on the rangeland water budget: Edwards Plateau, Texas. *Journal of the American Water Resources Association*, 41(1): 181-193.
- Agren, G.I., Franklin, O., 2003. Root : shoot ratios, optimization and nitrogen productivity. *Ann Bot*, 92(6): 795-800.
- Ameriflux. 2013. Ameriflux: Freeman Ranch woodland / US-FR3 [Online]. Available: <http://ameriflux.ornl.gov/fullsiteinfo.php?sid=97> [Accessed 10/24/2013].
- Ansley, R.J., Rasmussen, G.A., 2005. Managing native invasive juniper species using fire. *Weed Technology*, 19(3): 517-522.
- Anthoni, P.M., Law, B.E., Unsworth, M.H., 1999. Carbon and water vapor exchange of an open-canopied ponderosa pine ecosystem. *Agricultural and Forest Meteorology*, 95(3): 151-168.
- Arneth, A., Kelliher, F.M., McSeveny, T.M., Byers, J.N., 1998. Net ecosystem productivity, net primary productivity and ecosystem carbon sequestration in a *Pinus radiata* plantation subject to soil water deficit. *Tree Physiol*, 18(12): 785-793.
- Auken, O.W., McKinley, D.C., 2008. Structure and composition of *Juniperus* communities and factors that control them. In: Auken, O.W. (Ed.), *Western North American Juniperus Communities*. Ecological Studies. Springer, New York, pp. 19-47.
- Auken, O.W., Smeins, F., 2008. Western North American *Juniperus* communities: patterns and causes of distribution and abundance. In: Auken, O.W. (Ed.), *Western North American Juniperus Communities*. Ecological Studies. Springer, New York, pp. 3-18.
- Bai, Y.F., Wu, J.G., Xing, Q., Pan, Q.M., Huang, J.H. et al., 2008. Primary production and rain use efficiency across a precipitation gradient on the Mongolia plateau. *Ecology*, 89(8): 2140-2153.

- Baldocchi, D., 1994. A comparative study of mass and energy exchange over a closed C3 (wheat) and an open C4 (corn) canopy: II. CO<sub>2</sub> exchange and water use efficiency. *Agricultural and Forest Meteorology*, 67(3-4): 291-321.
- Baldocchi, D., 1997. Flux footprints within and over forest canopies. *Boundary-Layer Meteorology*, 85(2): 273-292.
- Baldocchi, D.D., 2003. Assessing the eddy covariance technique for evaluating carbon dioxide exchange rates of ecosystems: Past, present and future. *Global Change Biology*, 9(4): 479-492.
- Baldocchi, D.D., Black, T.A., Curtis, P.S., Falge, E., Fuentes, J.D. et al., 2005. Predicting the onset of net carbon uptake by deciduous forests with soil temperature and climate data: A synthesis of FLUXNET data. *International Journal of Biometeorology*, 49(6): 377-87.
- Barnes, P.W., Liang, S.-Y., Jessup, K.E., Ramirez, P.A., D'Souza, L.E. et al., 2008. Ecological impacts of Ashe juniper on subtropical savanna parklands and woodlands. In: Auken, O.W. (Ed.), *Western North American Juniperus Communities*. Ecological Studies. Springer, New York, pp. 133-155.
- Bartens, J., Grissino-Mayer, H.D., Day, S.D., Eric Wiseman, P., 2012. Evaluating the potential for dendrochronological analysis of live oak (*Quercus virginiana* Mill.) from the urban and rural environment—An explorative study. *Dendrochronologia*, 30(1): 15-21.
- Beer, C., Ciais, P., Reichstein, M., Baldocchi, D., Law, B.E. et al., 2009. Temporal and among-site variability of inherent water use efficiency at the ecosystem level. *Global Biogeochemical Cycles*, 23(2): 13.
- Bendevis, M.A., Owens, M.K., Heilman, J.L., McInnes, K.J., 2009. Carbon exchange and water loss from two evergreen trees in a semiarid woodland. *Ecophysiology*: 107-115.
- Binkley, D., Stape, J.L., Ryan, M.G., 2004. Thinking about efficiency of resource use in forests. *Forest Ecology and Management*, 193(1-2): 5-16.
- Black, K., Bolger, T., Davis, P., Nieuwenhuis, M., Reidy, B. et al., 2007. Inventory and eddy covariance-based estimates of annual carbon sequestration in a Sitka spruce (*Picea sitchensis* (Bong.) Carr.) forest ecosystem. *European Journal of Forest Research*, 126(2): 167-178.
- Blackard, J., Finco, M., Helmer, E., Holden, G., Hoppus, M. et al., 2008. Mapping U.S. forest biomass using nationwide forest inventory data and moderate resolution information. *Remote Sensing of Environment*, 112(4): 1658-1677.

- Bloom, A.J., Chapin, F.S., Mooney, H.A., 1985. Resource limitation in plants - an economic analogy. *Annual Review of Ecology and Systematics*, 16: 363-392.
- Buckland, S.T., Anderson, D.R., Burnham, K.P., Laake, J.L., 1993. Extensions and related work, In: *Distance Sampling: Estimating Abundance of Biological Populations*. Chapman and Hall, London, pp. 173-292.
- Burba, G.G., 2013. *Eddy Covariance Method for Scientific, Industrial, Agricultural and Regulatory Applications: A Field Book on Measuring Ecosystem Gas Exchange and Areal Emission Rates*. LI-COR Biosciences, Lincoln, NE, 331 pp.
- Cleaveland, M.K., 2000. A 963-year reconstruction of summer (JJA) streamflow in the White River, Arkansas, USA, from tree-rings. *The Holocene*, 10(1): 33-41.
- Cleaveland, M.K., 2006. *Extended Chronology of Drought in the San Antonio Area*. Guadalupe-Blanco River Authority and University of Arkansas, Fayetteville, 29 pp.
- Cleaveland, M.K., Cook, E.R., Stahle, D.W., 1992. Secular variability of the Southern Oscillation detected in tree-ring data from Mexico and the southern United States. In: Diaz, H.F., Markgraf, V. (Eds.), *El Niño: Historical and Paleoclimatic Aspects of the Southern Oscillation*. Cambridge University Press, Cambridge, UK, pp. 271-291.
- Cleaveland, M.K., Stahle, D.W., 1989. Tree-Ring analysis of surplus and deficit runoff in the White River, Arkansas. *Water Resources Research*, 25(6): 1391-1401.
- Cleaveland, M.K., Stahle, D.W., Therrell, M.D., Villanueva-Diaz, J., Burns, B.T., 2003. Tree-ring reconstructed winter precipitation and tropical teleconnections in Durango, Mexico. *Climatic Change*, 59(3): 369-388.
- Cleaveland, M.K., Votteler, T.H., Casteel, R.C., Stahle, D.K., Banner, J.L., 2011. Extended chronology of drought in south central, southeastern and west Texas. *Texas Water Journal*, 2(1): 54-96.
- Cook, E.R., 1985. *A Time Series Analysis Approach to Tree Ring Standardization*. Ph. D. Dissertation. The University of Arizona, Tucson, 171 pp.
- Cook, E.R., Meko, D.M., Stahle, D.W., Cleaveland, M.K., 1996. Tree-ring reconstructions of past drought across the coterminous United States: Tests of a regression method and calibration/verification results. In: Dean, J.S., Swetnam, T.W. (Eds.), *Tree Rings, Environment, and Humanity*. Proceedings of the International Conference, Department of Geosciences, University of Arizona, Tucson, pp. 155-169.

- Cook, E.R., Meko, D.M., Stahle, D.W., Cleaveland, M.K., 1999. Drought reconstructions for the continental United States. *Journal of Climate*, 12(4): 1145-1162.
- Curtis, P.S., Hanson, P.J., Bolstad, P., Barford, C., Randolph, J.C. et al., 2002. Biometric and eddy-covariance based estimates of annual carbon storage in five eastern North American deciduous forests. *Agricultural and Forest Meteorology*, 113(1-4): 3-19.
- Davidson, E.A., Savage, K., Bolstad, P., Clark, D.A., Curtis, P.S. et al., 2002. Belowground carbon allocation in forests estimated from litterfall and IRGA-based soil respiration measurements. *Agricultural and Forest Meteorology*, 113(1-4): 39-51.
- DeLucia, E.H., Drake, J.E., Thomas, R.B., Gonzalez-Meler, M., 2007. Forest carbon use efficiency: Is respiration a constant fraction of gross primary production? *Global Change Biology*, 13(6): 1157-1167.
- Diggle, P.J., 2003. *Statistical Analysis of Spatial Point Patterns*. Edward Arnold Publisher Ltd., London, 160 pp.
- Eggemeyer, K.D., Schwinning, S., 2009. Biogeography of woody encroachment: Why is mesquite excluded from shallow soils? *Ecohydrology*, 2(1): 81-87.
- Ehman, J.L., Schmid, H.P., Grimmond, C.S.B., Randolph, J.C., Hanson, P.J. et al., 2002. An initial intercomparison of micrometeorological and ecological inventory estimates of carbon exchange in a mid-latitude deciduous forest. *Global Change Biology*, 8(6): 575-589.
- Elkington, R.J., Rebel, K.T., Heilman, J.L., Litvak, M.E., Dekker, S.C. et al., 2014. Species-specific water use by woody plants on the Edwards Plateau, Texas. *Ecohydrology*, 7(2): 278-290.
- Falk, M., Wharton, S., Schroeder, M., Ustin, S., Paw, U.K., 2008. Flux partitioning in an old-growth forest: Seasonal and interannual dynamics. *Tree Physiol*, 28(4): 509-520.
- Fensholt, R., Rasmussen, K., Kaspersen, P., Huber, S., Horion, S. et al., 2013. Assessing land degradation/recovery in the African Sahel from long-term earth observation based primary productivity and precipitation relationships. *Remote Sensing*, 5(2): 664-686.
- Follansbee, R., 1994. *A History of the Water Resources Branch, U.S. Geological Survey; Volume I, from Predecessor Surveys to June 30, 1919*. US Geological Survey, Denver, 286 pp.

- Gao, Y., Zhu, X., Yu, G., He, N., Wang, Q. et al., 2014. Water use efficiency threshold for terrestrial ecosystem carbon sequestration in China under afforestation. *Agricultural and Forest Meteorology*, 195–196(0): 32-37.
- Gough, C.M., Vogel, C.S., Schmid, H.P., Su, H.B., Curtis, P.S., 2008. Multi-year convergence of biometric and meteorological estimates of forest carbon storage. *Agricultural and Forest Meteorology*, 148(2): 158-170.
- Granier, A., Biron, P., Kostner, B., Gay, L.W., Najjar, G., 1996. Comparisons of xylem sap flow and water vapour flux at the stand level and derivation of canopy conductance for Scots pine. *Theoretical and Applied Climatology*, 53(1-3): 115-122.
- Grissino-Mayer, H.D., 1993. An updated list of species used in tree-ring research. *Tree-Ring Bulletin*, 53: 17-43.
- Grissino-Mayer, H.D., 2001. Evaluating crossdating accuracy: A manual and tutorial for the computer program COFECHA. *Tree-Ring Research*, 57(2): 205-221.
- Hacke, U.G., Sperry, J.S., Wheeler, J.K., Castro, L., 2006. Scaling of angiosperm xylem structure with safety and efficiency. *Tree Physiol*, 26(6): 689-701.
- Ham, J.M., Heilman, J.L., 2003. Experimental test of density and energy-balance corrections on carbon dioxide flux as measured using open-path eddy covariance contribution no. 03-83-J from the Kansas Agric. Exp. Stn. *Agron. J.*, 95(6): 1393-1403.
- Hawley, F.M., 1937. Relationship of southern cedar growth to precipitation and run off. *Ecology*, 18(3): 398-405.
- Hedley, S.L., Buckland, S.T., 2004. Spatial models for line transect sampling. *Journal of Agricultural Biological and Environmental Statistics*, 9(2): 181-199.
- Heilman, J.L., Litvak, M.E., McInnes, K.J., Kjølgaard, J.F., Kamps, R.H. et al., 2014. Water-storage capacity controls energy partitioning and water use in karst ecosystems on the Edwards Plateau, Texas. *Ecohydrology*, 7(1): 127-138.
- Heilman, J.L., McInnes, K.J., Kjølgaard, J.F., Owens, M.K., Schwinning, S., 2009. Energy balance and water use in a subtropical karst woodland on the Edwards Plateau, Texas. *Journal of Hydrology*, 373(3-4): 426-435.
- Henshaw, F.F., Baldwin, G.C., Stevens, G.C., Fuller, E.S., 1915. Surface water supply of the United States, 1911 : Part 12. North Pacific Coast drainage basins. US Geological Survey, Washington, DC, 706 pp.

- Hsu, J.S., Powell, J., Adler, P.B., 2012. Sensitivity of mean annual primary production to precipitation. *Global Change Biology*, 18(7): 2246-2255.
- Huang, Y., Wilcox, B.P., 2005. How karst features affect recharge? Implication for estimating recharge to the Edwards Aquifer. In: Beck, B.F. (Ed.), 10th Multidisciplinary Conference on Sinkholes and the Engineering and Environmental Impact of Karst. American Society of Civil Engineers, San Antonio, TX, pp. 201-206.
- Hussain, M.Z., Grunwald, T., Tenhunen, J.D., Li, Y.L., Mirzae, H. et al., 2011. Summer drought influence on CO<sub>2</sub> and water fluxes of extensively managed grassland in Germany. *Agriculture Ecosystems & Environment*, 141(1-2): 67-76.
- Huxman, T.E., Smith, M.D., Fay, P.A., Knapp, A.K., Shaw, M.R. et al., 2004a. Convergence across biomes to a common rain-use efficiency. *Nature*, 429(6992): 651-4.
- Huxman, T.E., Snyder, K.A., Tissue, D., Leffler, A.J., Ogle, K. et al., 2004b. Precipitation pulses and carbon fluxes in semiarid and arid ecosystems. *Oecologia*, 141(2): 254-68.
- Inaba, N., Kondo, K., Numamoto, S., Hayashi, S., 2007. Influence of the definition of water-year period on discharge-duration analysis focused on low flow: In the case of the Tatsunokuchi-yama experimental watershed. *Journal of Japanese Forestry Society*, 89: 412-415.
- Jenkins, J.C., Chojnacky, D.C., Heath, L.S., Birdsey, R.A., 2003. National-scale biomass estimators for United States tree species. *Forest Science*, 49(1): 12-35.
- Jones, W.K., 2013. Physical structure of the epikarst. *Acta Carsologica*, 42(2-3): 311-314.
- Kim, J., Guo, Q., Baldocchi, D.D., Leclerc, M., Xu, L. et al., 2006. Upscaling fluxes from tower to landscape: Overlaying flux footprints on high-resolution (IKONOS) images of vegetation cover. *Agricultural and Forest Meteorology*, 136(3-4): 132-146.
- Kjelgaard, J.F., Heilman, J.L., McInnes, K.J., Owens, M.K., Kamps, R.H., 2008. Carbon dioxide exchange in a subtropical, mixed C3/C4 grassland on the Edwards Plateau, Texas. *Agricultural and Forest Meteorology*, 148(6-7): 953-963.
- Kljun, N., Black, T.A., Griffis, T.J., Barr, A.G., Gaumont-Guay, D. et al., 2006. Response of net ecosystem productivity of three boreal forest stands to drought. *Ecosystems*, 9(7): 1128-1144.

- Knight, R.W., Blackburn, W.H., Merrill, L.B., 1984. Characteristics of oak mottes, Edwards-Plateau, Texas. *Journal of Range Management*, 37(6): 534-537.
- Lauenroth, W.K., Burke, I.C., Paruelo, J.M., 2000. Patterns of production and precipitation-use efficiency of winter wheat and native grasslands in the central Great Plains of the United States. *Ecosystems*, 3(4): 344-351.
- Law, B.E., Sun, O.J., Campbell, J., Van Tuyl, S., Thornton, P.E., 2003. Changes in carbon storage and fluxes in a chronosequence of ponderosa pine. *Global Change Biology*, 9(4): 510-524.
- LiCor. 2013. EddyPro Software - LI-COR Environmental [Online]. Available: [http://www.licor.com/env/products/eddy\\_covariance/software.html](http://www.licor.com/env/products/eddy_covariance/software.html) [Accessed 09/23/2013].
- Luckman, B.H., 2007. Dendroclimatology. In: Elias, S.A. (Ed.), *Encyclopedia of Quaternary Sciences*. Elsevier, Oxford, UK, pp. 465-475.
- Luyssaert, S., Reichstein, M., Schulze, E.D., Janssens, I.A., Law, B.E. et al., 2009. Toward a consistency cross-check of eddy covariance flux-based and biometric estimates of ecosystem carbon balance. *Global Biogeochemical Cycles*, 23(3): 15.
- Massman, W.J., 2000. A simple method for estimating frequency response corrections for eddy covariance systems. *Agricultural and Forest Meteorology*, 104(3): 185-198.
- Massman, W.J., Lee, X., 2002. Eddy covariance flux corrections and uncertainties in long-term studies of carbon and energy exchanges. *Agricultural and Forest Meteorology*, 113(1-4): 121-144.
- Mauder, M., Foken, T., Clement, R., Elbers, J.A., Eugster, W. et al., 2008. Quality control of CarboEurope flux data; Part 2: Inter-comparison of eddy-covariance software. *Biogeosciences*, 5(2): 451-462.
- McCole, A.A., Stern, L.A., 2007. Seasonal water use patterns of *Juniperus ashei* on the Edwards Plateau, Texas, based on stable isotopes in water. *Journal of Hydrology*, 342(3-4): 238-248.
- McDowell, N., Pockman, W.T., Allen, C.D., Breshears, D.D., Cobb, N. et al., 2008. Mechanisms of plant survival and mortality during drought: Why do some plants survive while others succumb to drought? *New Phytol*, 178(4): 719-39.

- Meinzer, F.C., Woodruff, D.R., Eissenstat, D.M., Lin, H.S., Adams, T.S. et al., 2013. Above- and belowground controls on water use by trees of different wood types in an eastern US deciduous forest. *Tree Physiol*, 33(4): 345-56.
- Miller, G.R., 2009. Measuring and Modeling Interactions Between Groundwater, Soil Moisture, and Plant Transpiration in Natural and Agricultural Ecosystems. Ph. D. Dissertation. University of California, Berkeley, 243 pp.
- Miller, S.D., Goulden, M.L., Menton, M.C., da Rocha, H.R., de Freitas, H.C. et al., 2004. Biometric and micrometeorological measurements of tropical forest carbon balance. *Ecological Applications*, 14(4): S114-S126.
- Montgomery, R.A., Chazdon, R.L., 2002. Light gradient partitioning by tropical tree seedlings in the absence of canopy gaps. *Oecologia*, 131(2): 165-174.
- Morino, K.A., 2008. Using False Rings to Reconstruct Local Drought Severity Patterns on a Semiarid River. Ph. D. Dissertation. University of Arizona, Tucson, 132 pp.
- NCDC. 2014. Tree Ring Search [Online]. NOAA. Available: <http://hurricane.ncdc.noaa.gov/pls/paleox/f?p=518:1:0::APP:PROXYTOSEARCH:18> [Accessed 08/14/2014].
- Owens, M.K., 2008. Juniper tree impacts on local water budgets. In: Auken, O.W. (Ed.), *Western North American Juniperus Communities*. Ecological Studies. Springer, New York, pp. 188-201.
- Prince, S.D., De Colstoun, E.B., Kravitz, L.L., 1998. Evidence from rain-use efficiencies does not indicate extensive Sahelian desertification. *Global Change Biology*, 4(4): 359-374.
- Raich, J.W., Nadelhoffer, K.J., 1989. Belowground carbon allocation in forest ecosystems - global trends. *Ecology*, 70(5): 1346-1354.
- Randerson, J.T., Chapin, F.S., Harden, J.W., Neff, J.C., Harmon, M.E., 2002. Net ecosystem production: A comprehensive measure of net carbon accumulation by ecosystems. *Ecological Applications*, 12(4): 937-947.
- Rebmann, C., Gockede, M., Foken, T., Aubinet, M., Aurela, M. et al., 2005. Quality analysis applied on eddy covariance measurements at complex forest sites using footprint modelling. *Theoretical and Applied Climatology*, 80(2-4): 121-141.
- Reichstein, M. 2013. Online eddy covariance gap-filling and flux-partitioning tool. [Online]. Available: <http://www.bgc-jena.mpg.de/~MDIwork/eddyproc/upload.php> [Accessed 09/23/2013].

- Reichstein, M., Falge, E., Baldocchi, D., Papale, D., Aubinet, M. et al., 2005. On the separation of net ecosystem exchange into assimilation and ecosystem respiration: Review and improved algorithm. *Global Change Biology*, 11(9): 1424-1439.
- Reichstein, M., Tenhunen, J.D., Rouspard, O., Ourcival, J.-M., Rambal, S. et al., 2002. Severe drought effects on ecosystem CO<sub>2</sub> and H<sub>2</sub>O fluxes at three Mediterranean evergreen sites: Revision of current hypothesis? *Global Change Biology*, 8: 999-1017.
- Rocha, A.V., Goulden, M.L., Dunn, A.L., Wofsy, S.C., 2006. On linking interannual tree ring variability with observations of whole-forest CO<sub>2</sub> flux. *Global Change Biology*, 12(8): 1378-1389.
- Rosenzweig, M.L., 1968. Net primary productivity of terrestrial communities - prediction from climatological data. *American Naturalist*, 102(923): 67-74.
- Runyon, J., Waring, R.H., Goward, S.N., Welles, J.M., 1994. Environmental limits on net primary production and light-use efficiency across the Oregon transect. *Ecological Applications*, 4(2): 226-237.
- Russell, F.L., Fowler, N.L., 1999. Rarity of oak saplings in savannas and woodlands of the eastern Edwards Plateau, Texas. *Southwestern Naturalist*, 44(1): 31-41.
- Schmid, H.P., 2002. Footprint modeling for vegetation atmosphere exchange studies: A review and perspective. *Agricultural and Forest Meteorology*, 113(1-4): 159-183.
- Schotanus, P., Nieuwstadt, F.T.M., Debruin, H.A.R., 1983. Temperature-measurement with a sonic anemometer and its application to heat and moisture fluxes. *Boundary-Layer Meteorology*, 26(1): 81-93.
- Schwartz, B.F., Schwinning, S., Gerard, B., Kukowski, K.R., Stinson, C.L. et al., 2013. Using hydrogeochemical and ecohydrologic responses to understand epikarst process in semi-arid systems, Edwards Plateau, Texas, USA. *Acta Carsologica*, 42(2-3): 315-325.
- Schwinning, S., 2008. The water relations of two evergreen tree species in a karst savanna. *Oecologia*, 158(3): 373-83.
- Schwinning, S., Sala, O.E., Loik, M.E., Ehleringer, J.R., 2004. Thresholds, memory, and seasonality: Understanding pulse dynamics in arid/semi-arid ecosystems. *Oecologia*, 141(2): 191-3.

- Scott, R.L., 2010. Using watershed water balance to evaluate the accuracy of eddy covariance evaporation measurements for three semiarid ecosystems. *Agricultural and Forest Meteorology*, 150(2): 219-225.
- Scott, R.L., Edwards, E.A., Shuttleworth, W.J., Huxman, T.E., Watts, C. et al., 2004. Interannual and seasonal variation in fluxes of water and carbon dioxide from a riparian woodland ecosystem. *Agricultural and Forest Meteorology*, 122(1-2): 65-84.
- Slade, R.M., 1986. Large rainstorms along the Balcones Escarpment in central Texas. In: Abbott, P.L., Woodruff, C.M. (Eds.), *The Balcones Escarpment, Central Texas*. Geological Society of America, San Antonio, TX, pp. 15-20.
- Sperry, J.S., Nichols, K.L., Sullivan, J.E.M., Eastlack, S.E., 1994. Xylem embolism in ring-porous, diffuse-porous, and coniferous trees of northern Utah and interior Alaska. *Ecology*, 75(6): 1736-1752.
- Steinwand, A.L., Harrington, R.F., Or, D., 2006. Water balance for Great Basin phreatophytes derived from eddy covariance, soil water, and water table measurements. *Journal of Hydrology*, 329(3-4): 595-605.
- Taneda, H., Sperry, J.S., 2008. A case-study of water transport in co-occurring ring-versus diffuse-porous trees: Contrasts in water-status, conducting capacity, cavitation and vessel refilling. *Tree Physiol*, 28(11): 1641-51.
- Thomas, C.K., Law, B.E., Irvine, J., Martin, J.G., Pettijohn, J.C. et al., 2009. Seasonal hydrology explains interannual and seasonal variation in carbon and water exchange in a semiarid mature ponderosa pine forest in central Oregon. *Journal of Geophysical Research-Biogeosciences*, 114(G4): 22 pp.
- Tian, H., Chen, G., Liu, M., Zhang, C., Sun, G. et al., 2010. Model estimates of net primary productivity, evapotranspiration, and water use efficiency in the terrestrial ecosystems of the southern United States during 1895–2007. *Forest Ecology and Management*, 259(7): 1311-1327.
- Twine, T.E., Kustas, W.P., Norman, J.M., Cook, D.R., Houser, P.R. et al., 2000. Correcting eddy-covariance flux underestimates over a grassland. *Agricultural and Forest Meteorology*, 103(3): 279-300.
- Urbanski, S., Barford, C., Wofsy, S., Kucharik, C., Pyle, E. et al., 2007. Factors controlling CO<sub>2</sub> exchange on timescales from hourly to decadal at Harvard Forest. *Journal of Geophysical Research-Biogeosciences*, 112(G2): 25 pp.

- USEPA. 2013. Flow 101 [Online]. Available: <http://water.epa.gov/scitech/datait/models/dflow/flow101.cfm#year> [Accessed 12/3/2013].
- USGS. 2013. Explanations for the National Water Conditions [Online]. Available: <http://water.usgs.gov/wsc/glossary.html#W> [Accessed 12/03/2013].
- van Lanen, H.A.J., Fendekova, M., Kupczyk, E., Kasprzyk, A., Pokojski, W., 2004. Section 3.2.3 Water balance. In: Tallaksen, L.M., van Lanen, H.A.J. (Eds.), Hydrological Drought – Processes and Estimation Methods for Streamflow and Groundwater. Developments in Water Sciences. Elsevier, Amsterdam, pp. 64-65.
- Veni, G., 2013. A framework for assessing the role of karst conduit morphology, hydrology, and evolution in the transport and storage of carbon and associated sediments. *Acta Carsologica*, 42(2-3): 203-211.
- Vickers, D., Thomas, C.K., Pettijohn, C., Martin, J.G., Law, B.E. 2012. Five years of carbon fluxes and inherent water-use efficiency at two semi-arid pine forests with different disturbance histories [Online]. International Meteorological Institute in Stockholm, Stockholm. 64:(Feb 2012) 14 pp. Available: <http://www.tellusb.net/index.php/tellusb/article/view/17159> [Accessed 11/16/2014].
- Webb, E.K., Pearman, G.I., Leuning, R., 1980. Correction of flux measurements for density effects due to heat and water-vapor transfer. *Quarterly Journal of the Royal Meteorological Society*, 106(447): 85-100.
- White, P.B., van de Gevel, S.L., Grissino-Mayer, H.D., Laforest, L.B., Deweese, G.G., 2011. Climatic response of oak species across an environmental gradient in the southern Appalachian mountains, USA. *Tree-Ring Research*, 67(1): 27-37.
- Wilcox, B.P., 2002. Shrub control and streamflow on rangelands: A process based viewpoint. *Journal of Range Management*, 55(4): 318-326.
- Wilkinson, M., Eaton, E.L., Broadmeadow, M.S.J., Morison, J.I.L., 2012. Inter-annual variation of carbon uptake by a plantation oak woodland in south-eastern England. *Biogeosciences*, 9(12): 5373-5389.
- Wilson, K., Goldstein, A., Falge, E., Aubinet, M., Baldocchi, D. et al., 2002. Energy balance closure at FLUXNET sites. *Agricultural and Forest Meteorology*, 113(1-4): 223-243.
- Wink, R.L., Wright, H.A., 1973. Effects of fire on an Ashe juniper community. *Journal of Range Management*, 26(5): 326-329.

Zhu, X., Yu, G., Wang, Q., Hu, Z., Han, S. et al., 2013. Seasonal dynamics of water use efficiency of typical forest and grassland ecosystems in China. *Journal of Forest Research*, 19(1): 70-76.

## APPENDIX A

### VALIDATION STUDY

The pooled second Nearest Neighbor (NN<sub>2p</sub>) transect method was conducted along a single transect and involved only 20 study trees because of the time required to cut, transport and weigh trunks and leaves. This sparse data may have resulted in inaccurate estimates of tree density in the immediate area of the transect and may not adequately represent eddy covariance footprint area. Consequently, a plot-based density study to support the findings of Chapters II and V was undertaken several months after the main research had concluded. I did not have sufficient time and resources to create a statistically rigorous study and this should be viewed as an effort to detect egregious problems in Chapters II and V.

I chose 6 sites for the study as shown in figure A.1. The first was directly south of the tower and accessed by the tower driveway. The subsequent five were all accessed via the driveway described in Chapter II and which is known to Freeman Ranch staff as “Rusty’s Road.” Sites 4 and 5 were particularly close to the transect described in Chapter II and were used to validate the Nearest Neighbor method employed therein. Sites 1, 2, 3 and 6 were farther away from the transect and were used together with sites 4 and 5 to determine whether the data obtained from the transect was representative of the footprint area.

At each site, I used a roll of bright yellow twine to create a four-cornered polygon with roughly equal sides and 90 degree corners to approximate a square 400 m<sup>2</sup> survey plot. The sides and angles of the polygon were dictated to some extent by the

natural placement of the trees and brush at each location and it was difficult while working fast and alone to make exactly a square. Therefore, after the plot was created, I measured each side with a metric steel measuring tape and visually estimated the angles at each corner. Using these measurements, I calculated the actual area of each plot during post-processing. A GPS reading was recorded for each corner, but is only a general indicator of position because the GPS unit was not research-grade and returned values differing by 10 meters for the same location measured at different times. The GPS readings are presented in Table A.1. I then counted and recorded the species of every tree in each plot, recorded dbh (initially in inches, subsequently converted to cm) and assigned each tree to either the canopy group or the understory group in a manner similar to that used in Chapter II. Data are presented in Table A.2.

Values were transferred to a computer spreadsheet for post-processing. Density was calculated as the number of trees in a plot divided by the area of the plot. Separate values were calculated for canopy oaks, understory oaks, canopy junipers, understory junipers, canopy elms and understory elms. The final values are area weighted. In figure 2.3, the average annual radial increment for both the oaks and the junipers was approximately 1 mm. Therefore, biomass increment was estimated by first calculating the standing biomass based on equations in Chapter II, and then recalculating standing biomass after subtracting 2 mm from the diameter. In the absence of any dendrochronological data for this site regarding elm, the two equations in figure 2.4 were averaged and a 1 mm annual radial increment was assumed. I considered these

assumptions to be tolerable because elm only accounted for 4% of the canopy. The results of these calculations are presented in table A.3.

When the two plots closest to the transect (plots 4 and 5) are averaged together using areal weighting, a tree density of 748 ha<sup>-1</sup> results. This reasonably agrees with the transect-based NN2<sub>p</sub> estimation of tree density of 777 ha<sup>-1</sup>. The bootstrap modification of tree density at 807 ±160 ha<sup>-1</sup> easily contains both estimates within the range of its standard error of the mean, but the mean appears to be less accurate than the value of NN2<sub>p</sub>. In the broader scope of all plots in the study, the average tree density is yet lower at 650 ha<sup>-1</sup>, indicating that the transect was placed in a more dense part of the wooded area comprising the eddy covariance footprint. This is in conflict with the speculation in Chapter V that placement of the transect by a driveway biased the estimate toward lower density. The new, lower density estimate of canopy trees obtained by the plot-based method further emphasizes the role of the understory in the carbon and water cycles. However, it is notable that even the new estimate was within the error term of the bootstrap estimate. Also, critically, the estimate of the percentage of the NEP carbon budget (and, by extension, the water budget), remained 80% for oak and 20% for juniper due to the much larger sizes of the oaks. Therefore, after a new scaling factor was calculated and applied, the conclusions of Chapter V remained the same.

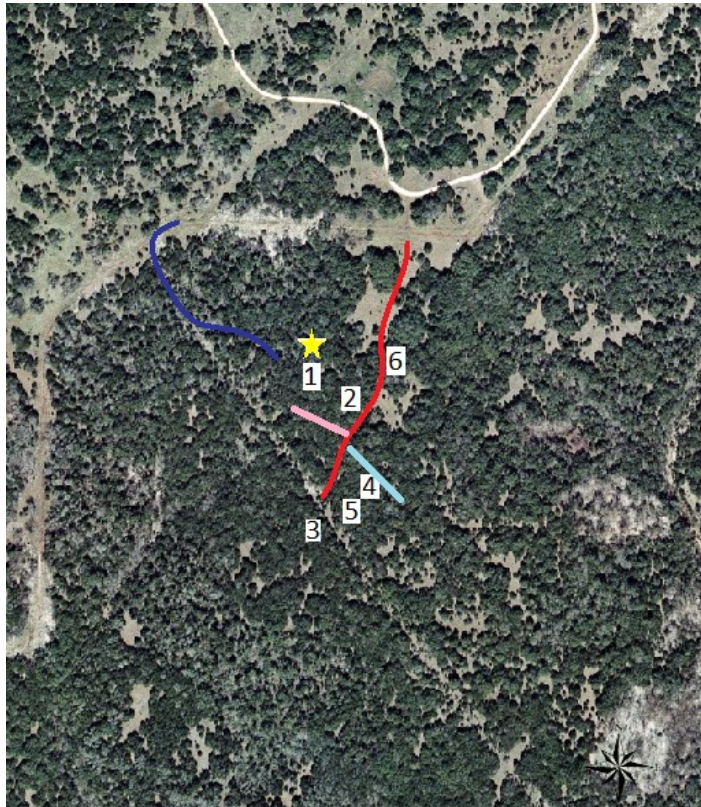


**Figure A.1 Map of the research site. The blue line is the driveway to the eddy covariance tower. The red line is “Rusty’s Road.” The gold star is the location of the eddy covariance tower. The pink and light blue lines mark the locations of the transects and the numbered squares represent the locations of the plots. Color imagery provided by Capital Area Council of Governments (CAPCOG) at: <http://www.capcog.org/data-maps-and-reports/geospatial-data/>**

**Table A.1 GPS coordinates for the research plots.**

Site number	First corner	Second corner	Third corner	Forth corner
1	29° 56.481' N 97° 59.634' W	29° 56.473' N 97° 59.610' W	29° 56.472' N 97° 59.652' W	29° 56.475' N 97° 59.649' W
2	29° 56.484' N 97° 59.609' W	29° 56.478' N 97° 59.615' W	29° 56.478' N 97° 59.620' W	29° 56.485' N 97° 59.617' W
3	29° 56.419' N 97° 59.661' W	29° 56.408' N 97° 59.653' W	29° 56.405' N 97° 59.654' W	29° 56.406' N 97° 59.658' W
4	29° 56.402' N 97° 59.599' W	29° 56.407' N 97° 59.592' W	29° 56.403' N 97° 59.583' W	29° 56.397' N 97° 59.586' W
5	29° 56.405' N 97° 59.628' W	29° 56.414' N 97° 59.617' W	29° 56.413' N 97° 59.611' W	29° 56.405' N 97° 59.610' W
6	29° 56.505' N 97° 59.594' W	29° 56.499' N 97° 59.598' W	29° 56.499' N 97° 59.588' W	29° 56.507' N 97° 59.586' W

**Table A.2 Tree density validation study results.**

	site 1	site 2	site 3	site 4	site 5	site 6	sum	density	density	canopy fraction
	count	m <sup>-2</sup>	ha <sup>-1</sup>	%						
Canopy Oak	8	15	2	8	18	13	64	0.0297	297	46
Understory Oak	4	9	0	3	3	3	22	0.0102	102	
Canopy Juniper	9	4	11	21	20	5	70	0.0325	325	50
Understory Juniper	33	40	16	37	42	13	181	0.084	840	
Canopy Elm	1	1	0	0	3	1	6	0.0028	28	4
Understory Elm	4	0	0	0	1	1	6	0.0028	28	
Canopy tree sum	18	20	13	29	41	19	140	0.065	650	
Area (m <sup>2</sup> )	343.8	420.5	219	417	479	275	2154.3			

**Table A.3 Biomass increment and canopy ratios validation study results.**

	oak	juniper	elm
average dbh (cm)	24.65	15.81	23.71
dbh Standard Deviation (cm)	9.42	7.87	5.94
dbh Maximum (cm)	76.2	50.29	27.94
dbh Minimum (cm)	10.16	5.08	12.7
biomass (Mg ha <sup>-1</sup> )	123.60	28.86	6.06
biomass after 2 mm reduction of dbh (Mg ha <sup>-1</sup> )	121.16	28.35	5.96
biomass increment (Mg ha <sup>-1</sup> )	2.44	0.51	0.10
biomass increment percentage of total	80	17	3
biomass increment percentage of oak and juniper	83	17	N/A

## APPENDIX B

### MONTHLY DATA VALUES

The paucity of raw data values presented in the dissertation may preclude future interested parties from expanding upon this work. The original raw data consists of roughly 13 billion values and is far too unwieldy to include herein. All of the calculations using eddy covariance were performed with 30 minute summary data which are available on the Ameriflux archive and freely available to access on the Internet, as noted in the methods sections and documented in References. However, given the changing nature of the Internet, a record of some useful values may still be helpful. . This appendix presents monthly data values in Table B.1.

**Table B.1. Monthly Data Values**

	Precipitation (mm)	ET (mm)	GPP (gm <sup>-2</sup> )	NEE (gm <sup>-2</sup> )
<b>2004</b>				
Aug	110.48	110.85	132.31	-42.23
Sep	96.87	95.39	146.70	-23.91
Oct	311.04	75.02	145.71	-8.69
Nov	357.78	42.93	96.56	-13.83
Dec	2.92	39.55	82.42	-26.26
<b>2005</b>				
Jan	69.65	46.82	64.59	-34.26
Feb	104.00	40.46	72.72	-16.46
Mar	84.24	67.67	142.30	-12.04
Apr	23.00	64.82	130.98	-18.17
May	126.03	93.77	163.81	-21.31
Jun	13.93	102.09	146.23	-65.06
Jul	154.22	93.58	203.89	5.29
Aug	45.36	104.70	153.11	-36.30
Sep	71.28	78.08	115.54	-8.72
Oct	41.80	43.39	74.17	-28.62
Nov	1.94	22.41	48.12	-28.47
Dec	2.92	13.32	27.30	-6.81
<b>2006</b>				
Jan	31.43	16.69	26.43	-10.78
Feb	23.00	25.78	35.95	-49.34
Mar	74.84	32.71	45.96	-34.24
Apr	82.62	59.73	135.23	-10.95
May	117.29	81.06	166.76	-40.95
Jun	85.21	78.73	138.23	-36.64
Jul	63.50	70.90	148.25	-30.15
Aug	3.56	22.73	61.17	8.61
Sep	101.28	35.34	92.72	-7.43
Oct	128.30	38.14	89.89	-17.80
Nov	12.64	34.55	77.32	-35.97
Dec	95.25	29.08	60.54	-48.55

**Table B.1. Continued.**

	Precipitation (mm)	ET (mm)	GPP (gm <sup>-2</sup> )	NEE (gm <sup>-2</sup> )
<b>2007</b>				
Jan	252.30	39.99	50.92	-26.53
Feb	2.27	34.07	60.78	-46.87
Mar	214.16	45.13	131.61	11.90
Apr	108.86	72.47	155.22	-31.25
May	195.37	105.51	200.90	-24.47
Jun	177.76	126.13	212.85	-98.23
Jul	427.67	119.02	258.43	-38.09
Aug	63.50	126.68	215.92	-24.18
Sep	62.21	101.96	170.44	-33.38
Oct	58.64	66.79	108.31	-43.22
Nov	23.98	41.76	64.35	-58.55
Dec	15.55	30.16	42.77	-33.19
<b>2008</b>				
Jan	23.65	26.61	27.37	-49.97
Feb	12.31	20.36	45.20	-28.85
Mar	107.24	33.08	73.22	-25.27
Apr	56.86	57.87	121.20	-24.66
May	14.90	56.77	179.34	-20.23
Jun	0.32	28.30	60.31	-10.58
Jul	69.98	53.76	96.95	-12.18
Aug	161.67	91.71	146.05	16.92
Sep	2.27	61.44	72.17	-33.52
Oct	0.00	23.47	35.32	-26.73
Nov	0.00	21.15	26.70	-8.94
Dec	0.00	20.31	19.37	-17.47

**Table B.1. Continued.**

	Precipitation (mm)	ET (mm)	GPP (gm <sup>-2</sup> )	NEE (gm <sup>-2</sup> )
<b>2009</b>				
Jan	11.73	21.63	28.82	5.47
Feb	38.04	26.91	55.77	-16.91
Mar	78.17	37.52	74.75	-22.92
Apr	112.39	54.16	110.34	-14.58
May	68.69	84.38	160.36	-39.86
Jun	39.20	64.52	101.10	-28.92
Jul	45.36	46.92	74.63	1.17
Aug	10.01	29.42	55.16	13.91
Sep	129.26	51.07	125.92	54.04
Oct	297.75	67.11	141.47	12.30
Nov	106.27	50.20	61.42	-68.97
Dec	52.16	31.85	47.25	-34.06
<b>2010</b>				
Jan	112.43	31.09	42.16	-36.38
Feb	101.57	41.51	32.11	-49.90
Mar	70.34	59.54	95.64	-46.64
Apr	64.80	79.99	119.32	-57.42
May	165.69	106.04	159.78	-38.38
Jun	132.91	105.01	154.58	-29.37
Jul	106.60	104.85	139.28	-29.61
Aug	9.72	85.49	105.26	-31.34
Sep	212.20	92.55	175.65	14.43
Oct	0.00	81.17	104.54	-65.91
Nov	14.90	34.87	54.22	-61.25
Dec	29.81	23.62	72.86	-27.98

**Table B.1. Continued.**

	Precipitation (mm)	ET (mm)	GPP (gm <sup>-2</sup> )	NEE (gm <sup>-2</sup> )
<b>2011</b>				
Jan	94.28	37.24	28.98	-98.88
Feb	16.20	30.87	1.97	-110.98
Mar	1.93	39.72	19.17	-106.81
Apr	0.65	38.54	60.65	-2.23
May	51.99	42.20	96.89	24.55
Jun	53.14	36.35	80.66	11.12
Jul	31.10	45.69	83.90	-12.57
Aug	0.32	18.35	41.04	13.68
Sep	24.30	18.83	24.76	20.29
Oct	62.86	46.55	127.97	11.92
Nov	67.39	30.92	83.52	-12.64
Dec	164.91	37.89	106.97	-2.77
<b>2012</b>				
Jan	86.57	28.25	50.26	-29.72
Feb	103.68	43.51	94.03	-24.16
Mar	150.98	63.44	125.51	-23.93
Apr	15.55	77.71	151.48	-36.92
May	208.33	99.59	153.80	-26.53
Jun	12.30	50.68	124.59	-44.25
Jul	93.63	61.72	39.83	-61.75
Aug	8.42	40.05	51.56	-36.35
Sep	145.80	70.22	68.97	-21.19
Oct	16.52	70.97	117.32	-44.64
Nov	1.30	35.42	85.26	-55.40
Dec	13.28	22.12	49.61	-11.04